DISCRETE AND CONTINUOUS
DYNAMICAL SYSTEMS SERIES B
Volume **23**, Number **2**, March **2018**

doi:10.3934/dcdsb.2018039

pp. **701–729**

CASCADES OF ALTERNATING SMOOTH BIFURCATIONS AND BORDER COLLISION BIFURCATIONS WITH SINGULARITY IN A FAMILY OF DISCONTINUOUS LINEAR-POWER MAPS

Laura Gardini*

Department of Economics, Society and Politics, University of Urbino
via Saffi 42, 61029 Urbino (PU), Italy

Roya Makrooni

Department of Mathematical Sciences, Sharif University of Technology, Tehran, Iran
Azadi St., Tehran, P.O.Box 11365-11155, Iran

Iryna Sushko

Institute of Mathematics, National Academy of Sciences of Ukraine
3 Tereshchenkivska st., 01601 Kyiv, Ukraine

(Communicated by Miguel Sanjuan)

Abstract. We investigate the dynamics of a family of one-dimensional linear-power maps. This family has been studied by many authors mainly in the continuous case, associated with Nordmark systems. In the discontinuous case, which is much less studied, the map has vertical and horizontal asymptotes giving rise to new kinds of border collision bifurcations. We explain a mechanism of the interplay between smooth bifurcations and border collision bifurcations with singularity, leading to peculiar sequences of attracting cycles of periods n, $2n$, $4n-1$, $2(4n-1)$,..., $n \geq 3$. We show also that the transition from invertible to noninvertible map may lead abruptly to chaos, and the role of organizing center in the parameter space is played by a particular bifurcation point related to this transition and to a flip bifurcation. Robust unbounded chaotic attractors characteristic for certain parameter ranges are also described. We provide proofs of some properties of the considered map. However, the complete description of its rich bifurcation structure is still an open problem.

1. **Introduction.** The large number of applied models characterized by sharp switching between different states are described by nonsmooth systems. The dynamics of such systems can often be investigated using a first return map defined on some Poincaré section of the phase space. This fact has lead to primary importance investigations of the bifurcations occurring in piecewise smooth maps, continuous or discontinuous, which expanded in the last decade. In particular, the well known Nordmark systems associated with grazing bifurcations have been intensively studied using one-dimensional (1D for short) piecewise smooth (PWS for short) return

2010 *Mathematics Subject Classification.* Primary: 37E05, 37G35; Secondary: 37N30.

Key words and phrases. Piecewise smooth maps, border collision bifurcations, cascade of smooth and nonsmooth bifurcations, skew tent map as a normal form, unbounded chaotic sets.

* Corresponding author: Laura Gardini.

maps with power function nonlinearities [21, 22]. In the present paper, we consider such a map, defined by two functions, $f_L(x)$ and $f_R(x)$, as follows:

$$x \mapsto f_\mu(x) = \begin{cases} f_L(x) = ax + \mu & \text{if} \quad x \le 0 \\ f_R(x) = bx^{-\gamma} + \mu & \text{if} \quad x > 0 \end{cases} \tag{1}$$

where a, b, μ, γ are real parameters and $\mu < 0$, $\gamma > 0$.

The PWS map (1) has been considered by many authors, mainly for $\gamma < 0$ corresponding to the continuous case. The most studied is the case $\gamma = -1/2$ related to the square-root nonlinearity, see [26, 23, 11, 5, 4, 3]. In [9, 7] the normal-form mapping of sliding bifurcations is derived, leading to an additional linear term in the function $f_R(x)$ in (1), and to the values $\gamma = -3/2$, $\gamma = -2$ and $\gamma = -3$, related to different cases of sliding bifurcations (see also [3]). Other examples of maps with nonlinear leading-order terms, associated with grazing and sliding bifurcations in power converters and in nonsmooth sliding-mode controls can be found in [5, 6, 1]. The piecewise linear case related to $\gamma = -1$ leads to the skew tent map, whose dynamics are well described (see, e.g., [14, 32, 34]). Map (1) with $\gamma = -2$ is a particular case of the linear-logistic map considered in [30, 31].

It is worth noticing that the power term in (1) in the applied context appears through a Taylor series expansion of a nonlinear function, and so it can take only particular positive values (as mentioned above). In all these cases the system is a continuous PWS map, whose characteristic feature is the occurrence of border collision bifurcations (BCB for short). This term, introduced by Nusse and Yorke (see [24, 25]) denotes the crossing of a border by an invariant set, typically a periodic point. The study of continuous PWS systems can take advantage of the skew tent map as a border collision normal form, a powerful analytical tool which allows to determine the effect of the border collision of cycles of any period. Applications can be found in [30, 31, 32, 33, 34], and we shall use it also in the present work.

Besides $\gamma < 0$, also the case $\gamma > 0$ has been recently analyzed for $\mu > 0$. This leads to a family of maps in which the function $f_R(x)$ has a vertical asymptote at the discontinuity point $x = 0$. The dynamic properties of such a family and bifurcations which can be observed under variation of its parameters are quite different from those occurring in the continuous case. The discontinuous case with $\gamma > 0$ is first considered in [27], and some remarks for the particular case with $\gamma = 1/2$ are reported in [28]. Detailed analysis of the discontinuous map in this case ($\mu > 0$) is presented in some recent papers ([15, 16, 17, 18, 19]), where several open problems are left for further investigations. In the present work we consider the discontinuous ($\gamma > 0$) map (1) for $\mu < 0$.

For a generic discontinuous map the complete classification of the possible results of a BCB is still an open problem, as well as the use of the piecewise linear map as a normal form. It concerns especially maps with a vertical asymptote giving rise to peculiar kinds of BCB. However, one of the main points in the investigation of PWS systems, especially discontinuous, is related to the fact that besides BCBs also standard bifurcations characteristic for smooth systems (we call them smooth bifurcations for short) may be involved in the bifurcation sequences. Thus, it is important to investigate the interactions between these two kinds of bifurcations. This is particularly relevant in maps with hyperbolic branches, that applies to the map considered in the present paper, and we shall explain how smooth and nonsmooth bifurcations alternate for some parameter ranges, leading to sequences of attracting cycles with peculiar periods.

The existence of a vertical asymptote in the applied models, particularly in engineering applications, is not new (see, e.g., [29], [13]). A peculiarity of such systems is associated with the fact that they can possess unbounded chaotic attractors. Such attractors are considered in [8] where they are related to structurally unstable situations, while in [16, 17] it is shown that in the discontinuous map (1) with $\mu > 0$ unbounded chaotic attractors exist and are robust, i.e. persistent under parameter perturbations in some open set in the parameter space. As we shall see, unbounded chaotic attractors of the map here considered, with $\mu < 0$, may be robust in some parameter regions and not robust in others.

The paper is organized as follows. In Sec.2 we first discuss an overall bifurcation structure of the parameter space of the considered map identifying the regions with nontrivial dynamics and splitting them in two parts, where the map is invertible ($a < 0,\ b < 0$) and noninvertible ($a < 0,\ b > 0$). Then, after the description of the bifurcations of the fixed points, we present the results associated with the dynamics of the map in the invertible case. We show that a *degenerate flip bifurcation* (DFB for short) of the fixed point occurs simultaneously with a *BCB with singularity* of a 4-cycle. Such a peculiarity is caused by the existence of the vertical and horizontal asymptotes of the map. This explains, in particular, a sharp transition from an attracting fixed point to an attracting 4-cycle. We describe also the flip bifurcation of the 2-cycle, which can be subcritical (for $0 < \gamma < 1$), degenerate (for $\gamma = 1$) and supercritical ($\gamma > 1$). Clearly, the noninvertible case is associated with more rich bifurcation structures which depend essentially on γ : our analysis is split in two parts, for $\gamma > 1$ and $0 < \gamma < 1$, described in Sec.3.1 and in Sec.3.2, respectively. The first case is characterized by particular sequences of alternating smooth and border collision bifurcations. In particular, using the skew tent map as a normal form and an auxiliary map, we show that smooth fold bifurcation (S-fold for short) and fold-BCB can occur, ultimately leading to a pair of cycles of map (1), one attracting and one repelling, whose periods differ by 1, say n and $(n-1)$, respectively. We show also that smooth flip bifurcation (S-flip for short) alternates either with flip-BCB or persistence-BC, so that starting from an attracting cycle of period n, a cascade of bifurcations leads ultimately to attracting cycles of periods $2n$, $(4n-1)$, $2(4n-1)$, $4(4n-1)-1$, ... that is, the period is alternatingly doubled and 'doubled-1'. In Sec.3.2 we show that for $0 < \gamma < 1$ the map may have attracting chaotic intervals, unbounded and robust, or chaotic repellors coexisting with an attracting fixed point or an attracting cycle. Sec.4 concludes.

2. **Preliminaries. invertible case** ($a < 0$, $b < 0$, $\gamma > 0$)**.** As mentioned in the Introduction, we are interested in the dynamics of map f_μ given in (1) in the case $\gamma > 0$, $\mu < 0$. Using the transformation $(x, a, b, \mu) \to (-x/\mu, a, b(-\mu)^{-\gamma-1}, -1)$ the parameter $\mu < 0$ can be scaled to $\mu = -1$, so that without loss of generality we can consider the map

$$x \mapsto f(x) = \begin{cases} f_L(x) = ax - 1 & \text{if} \quad x \le 0 \\ f_R(x) = bx^{-\gamma} - 1 & \text{if} \quad x > 0 \end{cases} \tag{2}$$

The overall bifurcation structure of the parameter space of map f is shown in Fig.1, where we present 2D bifurcation diagrams in the $(a, S(b))$-parameter plane for $0 < \gamma < 1$ (see Fig.1a) and for $\gamma > 1$ (see Fig.1b). Examples of map f are also shown (see Fig.1c). In the 2D bifurcation diagrams the values of the parameter b are scaled as $S(b) = \arctan(b)$. Given that the transformation S maps an unbounded interval $(-\infty, +\infty)$ into a bounded one, $(-\pi/2, \pi/2)$, one can see the bifurcation

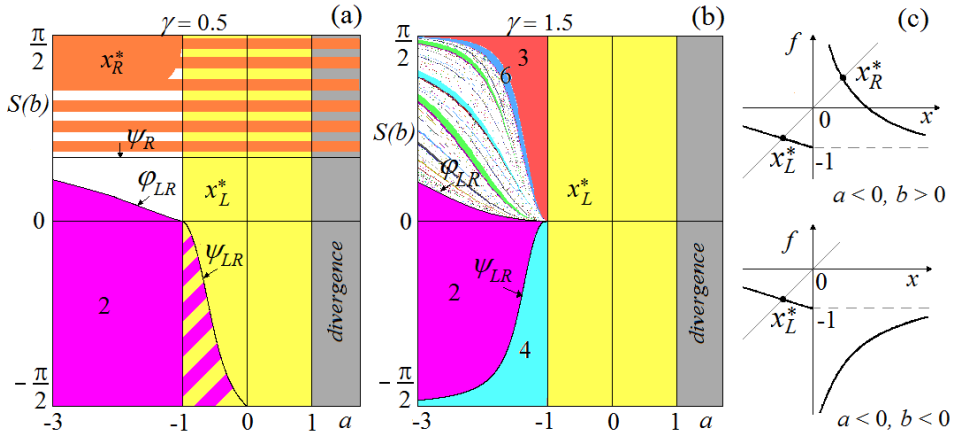

FIGURE 1. 2D bifurcation diagrams of f in the $(a, S(b))$-parameter plane, where $S(b) = \arctan(b)$, for $\gamma = 0.5$ in (a) and $\gamma = 1.5$ in (b); striped regions are related to coexistence, colored regions to attracting cycles of different periods, uncolored regions to attracting cycles of higher periods or chaotic attractors, grey regions to divergence. In (c) examples of map f are shown.

structure for the complete range of b, including the values tending to $-\infty$ and $+\infty$. The colored regions in Fig.1 are related to attracting cycles of period n, $n \le 60$, where different colors are associated with cycles of different periods; the gray region is related to divergent trajectories, the white region is related either to attracting cycles of higher periods or to chaotic attractors, and striped areas are related to coexistence.

In Fig.1 one can immediately see that the dynamics of f is much simpler for $b < 0$ than for $b > 0$. Moreover, the case $0 < \gamma < 1$ differs essentially from the case $\gamma > 1$. In fact, for $a < 0$, $b < 0$ map f is *invertible*, and, thus, it has rather simple dynamics which we completely describe below, in the present section. For $a < 0$, $b > 0$, map f is *noninvertible,* and thus its dynamics are more complicated. As one can see in Fig.1b (see also an enlargement in Fig.4a) the case $\gamma > 1$ is characterized by periodicity regions issuing from the point $(a, b) = (-1, 0)$ and related to the attracting cycles of peculiar periods, namely, for decreasing value of the parameter a one observes the adjacent regions of attracting cycles of periods n, $2n$, $4n-1$, $2(4n-1)$, ..., for $n \ge 3$. In the next section we explain the basic mechanism of such peculiar cascades. The case $0 < \gamma < 1$ (see Fig.1a) is characterized by unbounded robust chaos which may coexist with an attracting fixed point or an attracting cycle, as described in the next section as well. For completeness note that the case $a > 0$ is rather simple: for $\gamma > 1$ any trajectory is either attracted to the fixed point of map f_L or it diverges (see the yellow and gray regions, respectively, in Fig.1b), while for $0 < \gamma < 1$ also the fixed point of f_R may be attracting (see the orange striped region in Fig.1a).

To begin, let us denote two partitions of the definition range of map f as $I_L = (-\infty, 0]$, and $I_R = (0, +\infty)$, and its fixed points as $x = x_L^* \in I_L$, and $x = x_R^* \in I_R$.

To denote an n-cycle $\{x_i\}_{i=0}^{n-1}$ of map f we use its symbolic representation, associating the symbol L with $x_i \in I_L$, and R with $x_i \in I_R$. For example, an n-cycle

with $x_0 \in I_L$ and $x_i = f^i(x_0) \in I_R$, $i = 1, ..., n-1$, has the symbolic representation LR^{n-1}. With such a notation the point x_0 is related to the composite function $F_{LR^{n-1}}(x) = f_R^{n-1} \circ f_L(x)$ and is a solution of the equation $F_{LR^{n-1}}(x) = x$.

The fixed point $x_L^* = \frac{1}{a-1}$ exists obviously for $a < 1$; is attracting for $|a| < 1$; and at $a = -1$ it undergoes a degenerate flip bifurcation (DFB for short), at which any point of the set $[-1, 0] \setminus x_L^*$ is 2-periodic. The result of this bifurcation depends on the values of parameters b and γ, and we discuss it later. The fixed point x_R^* exists for $b > 0$; its bifurcations are described in the following

Proposition 1 (bifurcation of the fixed point x_R^*)**.** *Let $a \in \mathbb{R}$, $b > 0$ and $\gamma > 0$. Then map f given in (2) has a fixed point $x_R^* \in I_R$ satisfying $0 < x_R^* < b^{\frac{1}{\gamma}}$ which is repelling for $\gamma \geq 1$. For $0 < \gamma < 1$ a subcritical S-flip bifurcation of x_R^* occurs at*

$$b = \frac{\gamma^\gamma}{(1-\gamma)^{\gamma+1}} =: b_R^f \tag{3}$$

moreover,

$$x_R^*|_{b=b_R^f} = \frac{\gamma}{1-\gamma} =: x_{Rf}^* \tag{4}$$

The fixed point x_R^* is repelling for $0 < b \leq b_R^f$ and attracting for $b > b_R^f$.

Proof. It is easy to check that for $x > 0$ the function f_R is continuous, monotone decreasing and convex. From $\lim_{x\to 0^+} f_R(x) = +\infty$, $\lim_{x\to+\infty} f_R(x) = -1$, it follows that there is only one point, say x_R^*, satisfying $f_R(x_R^*) = x_R^*$, that is:

$$b - (x_R^*)^\gamma = (x_R^*)^{\gamma+1} \tag{5}$$

Moreover, it holds that $0 < x_R^* < O_R^{-1}$ where

$$O_R^{-1} := f_R^{-1}(0) = b^{\frac{1}{\gamma}} \tag{6}$$

From $f_R'(x) = \frac{-b\gamma}{x^{\gamma+1}} < 0$ and (5) it follows that

$$f_R'(x_R^*) = -\frac{b}{(x_R^*)^\gamma}\frac{\gamma}{x_R^*} = -\left(1 + \frac{1}{x_R^*}\right)\gamma \tag{7}$$

Since $(1 + \frac{1}{x_R^*}) > 1$ it holds that for $\gamma \geq 1$ the fixed point is repelling. Differently, for $0 < \gamma < 1$ the fixed point x_R^* may be attracting or repelling. Map f undergoes an S-flip bifurcation when $f_R'(x_{Rf}^*) = -1$, that is, when $(x_{Rf}^*)^{\gamma+1} = b\gamma$, or

$$x_{Rf}^* = (b\gamma)^{1/(\gamma+1)} \tag{8}$$

while from (7) it holds that $f_R'(x_R^*) \geq -1$ for $x_R^* \geq \frac{\gamma}{1-\gamma}$. Together with (8) this leads to $b\gamma \geq \left(\frac{\gamma}{1-\gamma}\right)^{\gamma+1}$. Thus $f_R'(x_R^*) \geq -1$ iff $b \geq b_R^f$, where b_R^f is the bifurcation value given in (3). Therefore, for $b > 0$ and $0 < \gamma < 1$ an S-flip bifurcation curve denoted ψ_R is defined as

$$\psi_R: \quad b = \frac{\gamma^\gamma}{(1-\gamma)^{\gamma+1}} \tag{9}$$

From (8) and (3) we also have that the fixed point at the flip bifurcation value is given by (4). The fixed point x_R^* is attracting for $b > b_R^f$, repelling for $b < b_R^f$, while for $b = b_R^f$ the fixed point x_{Rf}^* is repelling, because, as we prove below, the flip bifurcation is subcritical.

To investigate which kind of S-flip bifurcation of x_R^* occurs (subcritical, supercritical or degenerate) we check the sign of the third derivative of

$$f_R^2(x) = f_R \circ f_R(x) = \frac{b}{(bx^{-\gamma} - 1)^{\gamma}} - 1 \tag{10}$$

evaluated at the fixed point $x = x_{Rf}^*$ and at the bifurcation value $b = b_R^f$. Namely, (see, e.g., [36]), if $(f_R^2)'''(x_{Rf}^*) < 0$ (resp. > 0) then the flip bifurcation of the fixed point is *supercritical* (resp. *subcritical*). Using (4), we obtain

$$(f_R^2)'''(x_{Rf}^*) = \frac{1-\gamma^2}{(x_{Rf}^*)^2} = \frac{1}{\gamma^2}(1+\gamma)(1-\gamma)^3$$

from which we can conclude that for $0 < \gamma < 1$ it holds $(f_R^2)'''(x_R^*) > 0$ and thus the flip bifurcation is subcritical. □

Suppose now that $a < 0$, $b < 0$, so that map f is invertible. Below we prove several propositions describing the dynamics of f in such a case, indicating three qualitatively different cases, for $0 < \gamma < 1$, $\gamma > 1$ and $\gamma = 1$, illustrated in Fig.2a, b, and c, respectively.

Proposition 2 (bifurcations of the 2-cycle LR for $b < 0$)**.** *Let $a < 0$, $b < 0$ and $\gamma > 0$. Then map f given in (2) has a unique 2-cycle $\{x_0, x_1\}$ with $x_0 < \frac{1}{a} < 0$, $x_1 > 0$, which undergoes an S-flip bifurcation at*

$$\begin{array}{rcll} b & = & \dfrac{1}{a\gamma}\left(\gamma\dfrac{a+1}{1-\gamma}\right)^{\gamma+1} =: b_{LR}^f & \text{for} \quad \gamma \neq 1 \\ a & = & -1 & \text{for} \quad \gamma = 1 \end{array}$$

For $0 < \gamma < 1$ this S-flip bifurcation occurs at values $a \in (-1, 0)$, while for $\gamma > 1$ it occurs at values $a < -1$, moreover, it is subcritical for $0 < \gamma < 1$ and the 2-cycle is attracting for $b < b_{LR}^f$; supercritical for $\gamma > 1$ and the 2-cycle is attracting for $b \geq b_{LR}^f$; degenerate for $\gamma = 1$, and the 2-cycle is attracting for $a < -1$. Moreover, at $a = 0$ the 2-cycle LR disappears due to a BCB with singularity: $\{x_0, x_1\} \to \{-\infty, 0\}$ as $a \to 0_-$.

Proof. Let $\{x_0, x_1\}$ be the points of a 2-cycle of map f with symbolic sequence LR, and let $x_0 \in I_L$. Then it must hold that $x_0 < O_L^{-1} = f_L^{-1}(0) = \frac{1}{a}$ in order to have $x_1 = f_L(x_0) > 0$. The existence of a 2-cycle can be shown via the existence of a unique fixed point x_1 for the composite function

$$F_{RL}(x) := f_L \circ f_R(x) = \frac{ab}{x^{\gamma}} - (a+1) \tag{11}$$

For $x > 0$ the function $F_{RL}(x)$ is continuous, monotone decreasing and convex (since $F'_{RL}(x) = -\gamma\frac{ab}{x^{\gamma+1}} < 0$ and $F''_{RL}(x) > 0$). From $\lim_{x\to 0_+} F_{RL}(x) = +\infty$ and $\lim_{x\to+\infty} F_{RL}(x) = -(a+1)$ it follows that for any $a < 0$, the function $F_{RL}(x)$ intersects the diagonal in exactly one point, say $\overline{x}_1$, satisfying $F_{RL}(x) = x$, that is, $\overline{x}_1$ is a solution of the equation

$$\frac{ab}{x^{\gamma}} = x + a + 1 \tag{12}$$

Considering

$$F'_{RL}(x) = -\gamma\frac{ab}{x^{\gamma+1}} \tag{13}$$

by using (12) we obtain

$$F'_{RL}(\overline{x}_1) = -\gamma\left(1+\frac{a+1}{\overline{x}_1}\right) \tag{14}$$

The 2-cycle is attracting if $F'_{RL}(\overline{x}_1) > -1$, that is $-\gamma\left(1+\frac{a+1}{\overline{x}_1}\right) > -1$, leading to

$$\frac{a+1}{\overline{x}_1} < \frac{1}{\gamma} - 1 \tag{15}$$

From this inequality we can see that a sufficient condition for the 2-cycle to be attracting is $0 < \gamma \le 1$ and $a < -1$. Differently, for $\gamma > 1$ and $-1 < a < 0$ we have $(a+1) > 0$ while $(\frac{1}{\gamma} - 1) < 0$, so that the condition in (15) is not satisfied, leading to $F'_{RL}(\overline{x}) < -1$ and thus the 2-cycle is repelling. The transition attracting/repelling occurs when $F'_{RL}(\overline{x}_1) = -1$ and the 2-cycle undergoes an S-flip, i.e., from (13), when $-ab\gamma\overline{x}_1^{-(\gamma+1)} = -1$ holds. Thus

$$\overline{x}_1 = (ab\gamma)^{\frac{1}{\gamma+1}} \tag{16}$$

From (14) we also have $\overline{x}_1 = \gamma\left(\frac{a+1}{1-\gamma}\right)$ leading, at the flip bifurcation value, to

$$\overline{x}_1 = (ab\gamma)^{\frac{1}{\gamma+1}} = \gamma\left(\frac{a+1}{1-\gamma}\right) \tag{17}$$

The rightmost equation has solutions when both sides have the same sign, that is, for $b < 0$, $0 < \gamma < 1$ the flip bifurcation occurs at values $a \in (-1, 0)$, while for $\gamma > 1$ the flip bifurcation occurs at values $a < -1$. In both cases, the equation leads to the following flip bifurcation curve in explicit form:

$$\psi_{LR}: \quad b = \frac{1}{a\gamma}\left(\gamma\frac{a+1}{1-\gamma}\right)^{\gamma+1} =: b^f_{LR} \tag{18}$$

Moreover, from (15) we have $F'_{RL}(\overline{x}_1) > -1$ for $\frac{\overline{x}_1}{a+1} > \frac{\gamma}{1-\gamma}$, so that, for $0 < \gamma < 1$ (and thus $(a+1) > 0$) the stability condition holds for $\overline{x}_1 > \frac{\gamma(a+1)}{1-\gamma}$ leading to $b < b^f_{LR}$, while for $\gamma > 1$ (and thus $(a+1) < 0$) the stability condition holds for $\overline{x}_1 < \frac{\gamma(a+1)}{1-\gamma}$ leading to $b > b^f_{LR}$. Examples of the curve ψ_{LR} can be seen in Fig.1a,b.

The remaining case to consider is $\gamma = 1$. From (12) we have $x_1^2 + (a+1)x_1 - ab = 0$ leading to $\widetilde{x}_1 = 0.5(-(a+1) + \sqrt{(a+1)^2 + 4ab})$ and from (15) we have $F'_{RL}(\widetilde{x}_1) \ge -1$ iff $a \le -1$. Thus, the flip bifurcation of the 2-cycle occurs at $a = -1$, at which $\widetilde{x}_1 = \sqrt{-b}$. Moreover, at these parameter values ($\gamma = 1$ and $a = -1$), the function $F_{RL}(x)$ is linear-fractional:

$$\widetilde{F}_{RL}(x) = \frac{-b}{x} \tag{19}$$

and its derivative (from (13)) at the unique fixed point $\widetilde{x}_1 = \sqrt{-b}$ is always $\widetilde{F}'_{RL}(\widetilde{x}_1) = -1$ (for any b), while the second iterate of the function leads to the identity (that is $\widetilde{F}^2_{RL}(x) \equiv x$), which means that all the points of the interval $(0, +\infty)\backslash\widetilde{x}_1$ are 2-periodic for $\widetilde{F}_{RL}$ and thus 4-periodic for map f. It follows that for $\gamma = 1$ the flip bifurcation occurring at $a = -1$ is degenerate (see [32]), and for map f the 2-cycle is attracting (resp. repelling) for $a < -1$ (resp. $-1 < a < 0$).

The occurrence of a DFB for $\gamma = 1$ suggests that for $\gamma > 1$ and $\gamma < 1$ the type of flip bifurcation of the 2-cycle changes. To see in which way we consider the sign of the third derivative of the second iterate of $F_{RL}(x)$ in (11), that is of the function

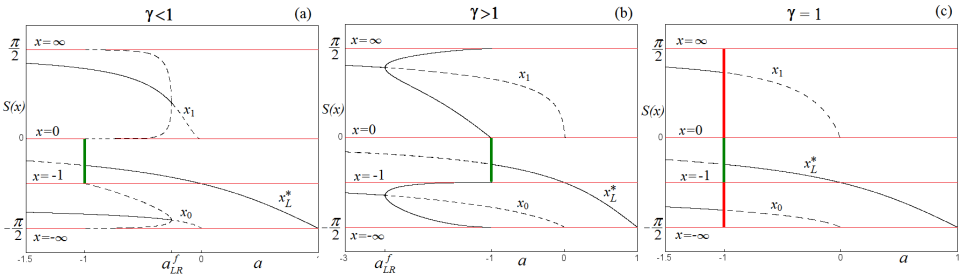

FIGURE 2. Bifurcation diagrams a vs $S(x)$ at $b = -5$, where $S(x) = \arctan(x)$. In (a) $\gamma = 0.5$, in (b) $\gamma = 2$ and in (c) $\gamma = 1$, associated with the subcritical, supercritical and degenerate flip bifurcations of the 2-cycle LR, respectively.

$F^2_{RL}(x) = F_{RL} \circ F_{RL}(x)$, evaluated at the fixed point $\overline{x}_1$ given in (17), and at the bifurcation values given in (18):

$$(F^2_{RL})'''(\overline{x}_1) = \frac{1-\gamma^2}{(\overline{x}_1)^2} \tag{20}$$

For $0 < \gamma < 1$ it holds $(F^2_{RL})'''(\overline{x}_1) > 0$ and thus the flip bifurcation of the 2-cycle is *subcritical* (see Fig.2a), while for $\gamma > 1$ it is *supercritical* (see Fig.2b).

As a result, we have that for any $\gamma \gtreqless 1$ and fixed $b < 0$, besides the attracting fixed point x^*_L a unique repelling 2-cycle LR exists as $a \to 0_-$, while it does not exist for $a > 0$ (when the fixed point x^*_L is globally attracting). Indeed, crossing $a = 0$ the fixed point x^*_L does not change its stability. However, the map changes from invertible to noninvertible, and the value $a = 0$ also corresponds to a BCB with singularity of the 2-cycle LR which becomes repelling after the flip bifurcation (necessarily occurring increasing the value of a from $-\infty$ to 0). In fact, the points of the 2-cycle are given by $\{f_R(\epsilon), \epsilon\}$, with $\epsilon > 0$ approaching 0 and, thus, $f_R(\epsilon)$ approaching $-\infty$. At $a = 0$, due to the flat branch $f_L(x)$ the 2-cycle disappears (or we may consider that it becomes $\{-\infty, 0\}$) and it does not exist for $a > 0$. □

Considering the results stated in Propositions 1 and 2 we can completely describe the dynamics of f in the particular case $\gamma = 1$ (see Fig.2c).

Proposition 3 (DFB of the 2-cycle)**.** *Let $a < 0$, $b < 0$ and $\gamma = 1$. Then for map f given in (2) it holds that for $-1 < a < 0$ the fixed point x^*_L is attracting and the 2-cycle LR appearing at $a = 0$ is repelling; for $a = -1$ the segment $[-1, 0]\backslash x^*_L$ is filled with 2-cycles, while the segments $(-\infty, -1)\backslash x_0$ and $(0, +\infty)\backslash x_1$ are filled with 4-cycles; for $a < -1$ the fixed point x^*_L is repelling and the 2-cycle LR is attracting.*

Regarding the flip bifurcation of the 2-cycle RL proved so far, in the subcritical case, i.e. for $0 < \gamma < 1$, at fixed $b < 0$, as the parameter a is decreased from $a = 0$, at a value $a^f_{LR} \in (-1, 0)$ the subcritical flip bifurcation occurs (for fixed values of b and γ the value a^f_{LR} is obtained from the equation of ψ_{LR} given in (15)). It leads to an attracting 2-cycle LR and a repelling 4-cycle $(RL)^2$. Thus, for a range of values of the parameter a we have bistability: for $a \in (-1, a^f_{LR})$ the fixed point x^*_L and the 2-cycle LR are both attracting. The basin of attraction of the 2-cycle is bounded by the 4-periodic points of the repelling 4-cycle. The other points converge to x^*_L. At $a = -1$ the DFB of x^*_L occurs at which any point of the interval $[-1, 0]\backslash x^*_L$ is

2-periodic, but the 2-cycle $\{0,-1\}$ on the boundary can also be considered as a 4-cycle $\{0,-\infty,+\infty,-1\}$, and in fact it corresponds to the BCB with singularity of the repelling 4-cycle, which does not exist for $a<-1$, when x_L^* becomes repelling and the 2-cycle LR globally attracting (except for x_L^*). The bifurcation sequence in the subcritical case is shown in Fig.2a.

Fig.2b illustrates the bifurcations occurring in the supercritical case, i.e. for $\gamma>1$. Considering some fixed values of $\gamma>1$ and $b<0$, as the parameter a is increased from $-\infty$ we have the repelling fixed point x_L^* and the globally attracting (except for x_L^*) 2-cycle LR. This holds up to the flip bifurcation value $a_{LR}^f<-1$, at which a supercritical flip bifurcation occurs, leading to a repelling 2-cycle LR and an attracting 4-cycle $(LR)^2$. In the interval $a\in(a_{LR}^f,-1)$ the 4-cycle attracts all the points except for the unstable 2-cycle and the unstable fixed point x_L^*. At $a=-1$ the DFB of x_L^* occurs (the segment $[-1,0]\backslash x_L^*$ is filled with 2-cycles). The 2-cycle $\{0,-1\}$ on the boundary can also be considered as a 4-cycle $\{0,-\infty,+\infty,-1\}$, and in fact it corresponds to the BCB with singularity of the attracting 4-cycle, which does not exist for $a>-1$, when x_L^* becomes attracting. For $a\in(-1,0)$ the fixed points x_L^* attracts all the points except for the unstable 2-cycle LR.

The BCB of the unstable 2-cycle is described in Proposition 2, while the arguments presented above describe the BCB of the 4-cycle, as summarized in the following

Proposition 4 (BCB of the 4-cycle $(RL)^2$)**.** *Let $a<0$, $b<0$, $\gamma>0$. Then for map f given in (2) at $a=-1$ a BCB with singularity occurs so that for $0<\gamma<1$ the repelling 4-cycle disappears as $a\to-1_+$; for $\gamma>1$ the attracting 4-cycle disappears as $a\to-1_-$.*

3. **Dynamics in the noninvertible case** ($a<0$, $b>0$, $\gamma>0$)**.** First note that for $a=-1$, $b>0$, in the segment $[-1,0]\backslash x_L^*$ filled with 2-cycles (related to the DFB of the fixed point x_L^*), the border 2-cycle $\{x_0,x_1\}|_{a=-1}=\{0,-1\}$ can be considered as a 3-cycle $\{x_0,x_1,x_2\}|_{a=-1}=\{0,+\infty,-1\}$. In fact, as a is decreasing through -1, a 3-cycle LR^2 appears due to a BCB with singularity. Below we prove that for $a<-1$, at least for $a=-1-\varepsilon$, for some $\varepsilon>0$, this 3-cycle LR^2 is attracting for $\gamma>1$, while it is repelling (and belonging to a chaotic attractor) for $\gamma<1$.

Since for $a<0$, $b>0$ both functions $f_L(x)$ and $f_R(x)$ are decreasing, we have that besides a BCB, a cycle of f of *odd* period may undergo an S-flip bifurcation because it has a negative eigenvalue, while a cycle of f of *even* period may undergo an S-fold bifurcation, given that it has a positive eigenvalue.

Let us now introduce an auxiliary map defined by three functions, $f_L(x)$, $f_M(x)=f_R^2(x)$, and $f_R(x)$, which is of help to study the dynamics of map f for some parameter ranges.

Proposition 5 (map g)**.** *Let $b>0$, $\gamma>0$. Then the dynamics of map f given in (2) are in one-to-one correspondence with the dynamics of the map g defined as*

$$x\mapsto g(x)=\begin{cases} f_L(x)=ax-1 & \text{if} \quad x\le 0 \\ f_M(x)=\frac{b}{(bx^{-\gamma}-1)^{\gamma}}-1 & \text{if} \quad 0<x<O_R^{-1}=b^{\frac{1}{\gamma}} \\ f_R(x)=bx^{-\gamma}-1 & \text{if} \quad x\ge O_R^{-1} \end{cases} \tag{21}$$

which is continuous at $x=0$, with $g(0)=-1$, and discontinuous at $x=O_R^{-1}$ with $\lim_{x\to(O_R^{-1})_-}g(x)=+\infty$ and $\lim_{x\to(O_R^{-1})_+}g(x)=0$.

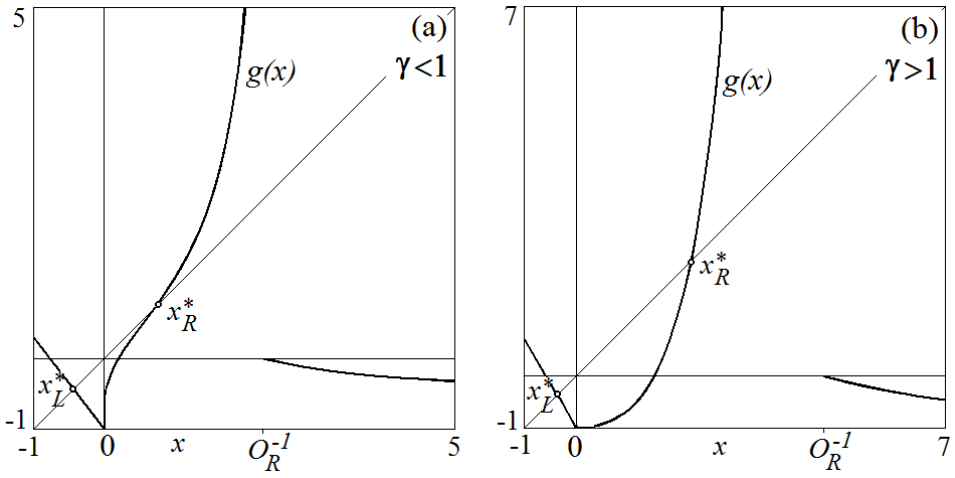

FIGURE 3. Graph of map $g(x)$ given in (21). In (a): $a = -1.3$, $b = 1.5$ and $\gamma = 0.5 < 1$; in (b) $a = -1.7$, $b = 10$ and $\gamma = 1.5 > 1$.

Proof. For $b > 0$ any point $x > O_R^{-1}$ is mapped by $f_R(x)$ in one iteration to I_L, while any point $0 < x < O_R^{-1}$ has a trajectory which starts with the symbolic sequence R^2. This implies that the dynamic behavior of map f can be equivalently studied by using the map $g(x)$ defined above. Moreover, from $\lim_{x\to 0_+} f_R(x) = +\infty$ and $\lim_{x\to+\infty} f_R(x) = -1$ it follows $\lim_{x\to 0_+} g(x) = \lim_{x\to 0_+} f_M(x) = -1$, thus the function $g(x)$ is continuous in $x = 0$, while it is discontinuous in $x = O_R^{-1}$ with $\lim_{x\to(O_R^{-1})_-} g(x) = \lim_{x\to(O_R^{-1})_-} f_M(x) = +\infty$ and $\lim_{x\to(O_R^{-1})_+} g(x) = f_R(O_R^{-1}) = 0$. □

The middle branch $f_M(x)$ is monotone increasing for $0 < x < O_R^{-1}$ as follows from the positive derivative:

$$\frac{d}{dx} f_R^2(x) = f_R'(f_R(x)) f_R'(x) = \frac{b^2\gamma^2}{(b - x^\gamma)^{\gamma+1}} x^{\gamma^2-1} > 0$$

since $(b - x^\gamma) > 0$ holds for $x \in (0, O_R^{-1})$, so we have $g'(x) > 0$, and it is easy to see that

$$\lim_{x\to 0_+} g'(x) = \begin{cases} 0 & \text{if } \gamma > 1 \\ 1 & \text{if } \gamma = 1 \\ +\infty & \text{if } 0 < \gamma < 1 \end{cases} \tag{22}$$

Moreover, for $\gamma \geq 1$ the function $f_M(x)$ is convex, since $g''(x) > 0$ holds. For $\gamma < 1$ it holds that $g''(\widetilde{x}) = 0$ where $\widetilde{x}$ is the inflection point:

$$\widetilde{x} = b^{\frac{1}{\gamma}}(1 - \gamma)^{\frac{1}{\gamma}} \tag{23}$$

so that the function $f_M(x)$ is concave for $0 < x < \widetilde{x}$ while it is convex for $\widetilde{x} < x < b^{\frac{1}{\gamma}}$ (and clearly at the bifurcation value $b = b_R^f$ (see (3)) the inflection point corresponds to the fixed point, i.e. $\widetilde{x} = x_{Rf}^*$). Examples of map $g(x)$ are shown in Fig.3.

It is plain that given the symbolic sequence of a trajectory of map g, that is a sequence in which the three symbols L, M and R may occur, to obtain the symbolic sequence of the corresponding trajectory of map f it is enough to replace the symbol M with R^2.

Recall that in the interval $[-1, O_R^{-1})$ the PWS map $g(x)$ is unimodal with a local minimum in the kink point $x = 0$, thus $x = 0$ is a local extremum for any composite function $g^n(x)$, $n \geq 1$, and the following property holds:

Property 1. *Let $a < 0$, $b > 0$ and $\gamma > 0$, then for any $n > 1$ the function $g^n(x)$ satisfies*

$$\lim_{x\to 0_+} \frac{d}{dx} g^n(x) = \begin{cases} 0 & \text{if } \gamma > 1 \\ +\infty & \text{if } 0 < \gamma < 1 \text{ and } g^n(0) \text{ is a local minimum} \\ -\infty & \text{if } 0 < \gamma < 1 \text{ and } g^n(0) \text{ is a local maximum} \end{cases} \tag{24}$$

This property immediately follows from the value of the derivative of $g^n(x)$ for $n = 1$ (as given in (22)) by applying the chain rule for the derivative. For $\gamma > 1$ the derivative is always zero, for any n. Similarly for $0 < \gamma < 1$ the derivative is always infinite, and the sign depends on the local minimum or local maximum of the function $g^n(x)$ at $x = 0$.

Notice that as long as the inequality $f_L(-1) = -a - 1 < x_R^*$ holds, the dynamics of the PWS map $g(x)$ can be restricted to an invariant absorbing interval $J \subset [-1, O_R^{-1})$.

Property 2. *Let $\gamma > 0$ and $a < -1$, then map g is continuous and unimodal in the invariant absorbing interval J defined as follows:*

1. *when x_R^* is repelling (see Proposition 1) and $b = b_R^h$, where*

$$b_R^h := -a(-a-1)^\gamma \tag{25}$$

   and the first homoclinic bifurcation of x_R^* occurs, then $J = [-1, -1-a] = [-1, x_R^*]$;
2. *when x_R^* is repelling and $b > b_R^h$ then $J = [-1, -1-a] \subset [-1, x_R^*]$;*
3. *when x_R^* is attracting and $b > b_R^h$, then $J = [-1, x_R^*]$.*

To see that this property holds, recall first that the invariant absorbing interval is determined by the iterates of the local extremum, that is, we have to consider the interval $[g(0), g^2(0)] = [-1, -a-1]$. Clearly, when the fixed point x_R^* is repelling, then as long as the inequality $f_L(-1) = -a - 1 < x_R^*$ holds, the dynamics of the PWS map $g(x)$ can be restricted to the interval $J = [-1, -1-a] \subset [-1, x_R^*]$. In fact, any point belonging to the interval $(-a-1, x_R^*)$ has the trajectory entering J in a finite number of iterations. Moreover, any point of the interval (x_R^*, O_R^{-1}) is mapped to $x > O_R^{-1}$ in a finite number of iterations while any point belonging to the interval $[O_R^{-1}, +\infty)$ is mapped to $x \leq 0$ in J in one iteration.

When the fixed point x_R^* is attracting, then as long as it holds $f_L(-1) = -a-1 < x_R^*$, the dynamics of the PWS map $g(x)$ can be restricted to $J = [-1, x_R^*]$, which is invariant ($g(J) = J$) and any point belonging to the interval $(x_R^*, +\infty)$ is mapped in J in a finite number of iterations or converges to x_R^*.

So we have to detect when the condition $-a-1 \leq x_R^*$ holds. Given that x_R^* must satisfy $f_R(x) = x$, i.e. $bx^{-\gamma} - 1 = x$, we have $-a - 1 \leq b{x_R^*}^{-\gamma} - 1$ leading to $b \geq b_R^h$ where b_R^h is given in (25). When the fixed point x_R^* is repelling, the equation $b = b_R^h$ corresponds to the curve in the (a, b)-parameter plane (for fixed γ) at which the *first homoclinic bifurcation* of x_R^* occurs. In fact, for $b > b_R^h$ the fixed point x_R^* has no rank-1 preimage in J (since $f_L^{-1}(x_R^*) < -1$). At $b = b_R^h$ we have $-1 \in g^{-1}(x_R^*)$, i.e. $0 \in g^{-2}(x_R^*)$, and infinitely many critical homoclinic orbits of x_R^* exist. For $b > b_R^h$ infinitely many noncritical homoclinic orbits of x_R^* exist (see e.g. [10]).

One more relevant change in the dynamics of map f occurring when $a < -1$, besides the homoclinic bifurcation at $b = b_R^h$, is related to the crossing of the discontinuity point of map g by the value $f_L(-1)$, that is when $f_L(-1) = O_R^{-1}$, separating the cases in which $f_L(-1) \lesseqgtr O_R^{-1}$, and only for $f_L(-1) > O_R^{-1}$ it is possible to have cycles of f with periodic points in $x < 0$ and $x > O_R^{-1}$. In particular, it is possible for map f to have a new pair of 2-cycles LR, as we shall see in Sec.3.1.4. Given that $f_L(-1) \geq O_R^{-1}$ holds for $-a-1 \geq b^{\frac{1}{\gamma}}$, that is, for $b \leq (-a-1)^\gamma$, we have that in the parameter space the boundary of the region has the following equation:

$$b = (-a-1)^\gamma =: b_{LR^3} \tag{26}$$

and corresponds to the BCB of a cycle of map f. In fact, when $f_L(-1) = O_R^{-1}$ we have the repeated sequence $\{0, -1, O_R^{-1}\}$. Noticing that for $a < -1$ and $b > (-a-1)^\gamma$ a 3-cycle with symbolic sequence L^2R cannot exist, it must be the BCB of a 4-cycle LR^3, existing for $b > (-a-1)^\gamma$, which becomes $\{0, +\infty, -1, O_R^{-1}\}$ at the border collision leading to a 3-cycle with symbolic sequence L^2R for $b < (-a-1)^\gamma$.

We can describe now the role of the bifurcation curves $b = b_R^h$ given in (25) and $b = b_{LR^3}$ given in (26) for the symbolic sequences which are allowed for map f. Keeping fixed a value of $b > 0$ and considering the parameter a in the range $a \in (a_h^R, -1)$ (where a_h^R and b satisfy the equation of b_R^h) the asymptotic dynamics of map g involve only the symbols L and M (and thus L and R^2 for map f). Differently, at smaller values of a, in the range $a \in (a_{LR^3}, a_R^h)$ (where a_{LR^3} and b satisfy the equation of b_{LR^3}) the asymptotic dynamics of map g involve all the symbols L, M, and R, but L is necessarily followed by M (that is, for map f the symbol L is necessarily followed by R^2), and since M may be followed by M or R we have that for map f the symbol L is necessarily followed by at least R^3. For $a < a_{LR^3}$ also the sequence of symbols LRL is allowed, both for map g and map f.

For any $\gamma > 0$ the interesting dynamic behaviors which occur for $a < -1$, when map f is noninvertible, differ depending on $\gamma \lesseqgtr 1$ as can be seen in Fig.1a,b, and the difference is due to the property of map g in the right neighborhood of $x = 0$: with slope 0 (resp. $+\infty$) for $\gamma > 1$ (resp. $\gamma < 1$). These two cases are considered separately, in Sec.3.1 and Sec.3.2.

3.1. **Periodicity regions** ($a < -1,\ b > 0,\ \gamma > 1$)**.** In the considered parameter range, several periodicity regions related to attracting cycles exist, while the fixed point x_R^* is always repelling, as well as x_L^*. An enlargement of Fig.1b is shown in Fig.4a in the (a, b)-parameter plane. The periodicity regions are better visible for larger values of γ (see Fig.4b). Here different colors are related to attracting cycles of different periods. As one can see, the periodicity regions issue from the point $(a, b) = (-1, 0)$, which is an intersection point of two straight lines, the one given by $a = -1$ associated with the DFB of the fixed point x_L^*, and another one defined by $b = 0$, related to the transition from invertibility to noninvertibility of map f. The curves b_R^h and b_{LR^3} given in (25) and (26), respectively, are also shown. On the right side of the curve b_R^h we can see a sequence of adjacent periodicity regions related to attracting cycles of map f of periods 1, 3, 6, 11, ... or 5, 10, 19, ... Below we explain why such peculiar periods are observed.

At any fixed value $b > 0$, decreasing the parameter a through -1 the fixed point x_L^* undergoes a DFB, leading to a unique attracting 3-cycle. In fact, as shown in Fig.3b, in the interval J in which map g is unimodal, this bifurcation leads (for $a = -1 - \varepsilon$, for sufficiently small $\varepsilon > 0$) to a 2-cycle with symbolic sequence LM,

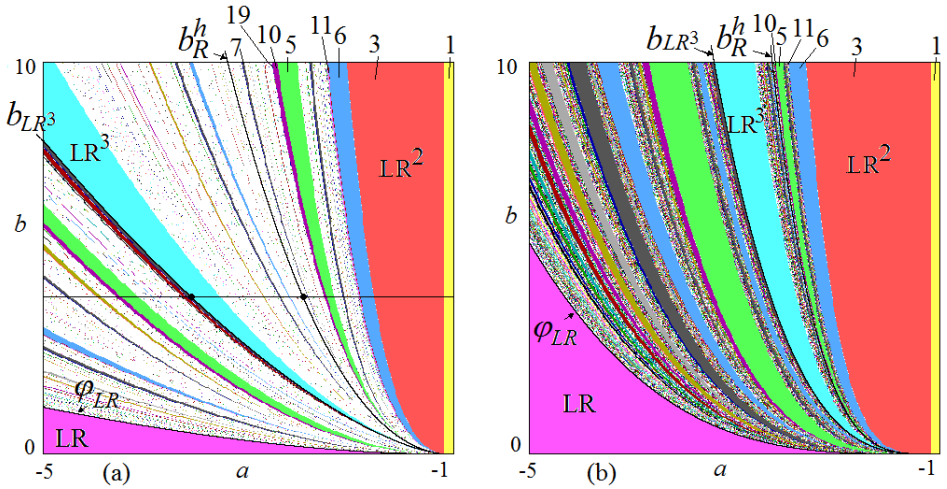

FIGURE 4. 2D bifurcation diagrams of map f in the (a, b)-parameter plane for $\gamma = 1.5$ in (a) and $\gamma = 3$ in (b).

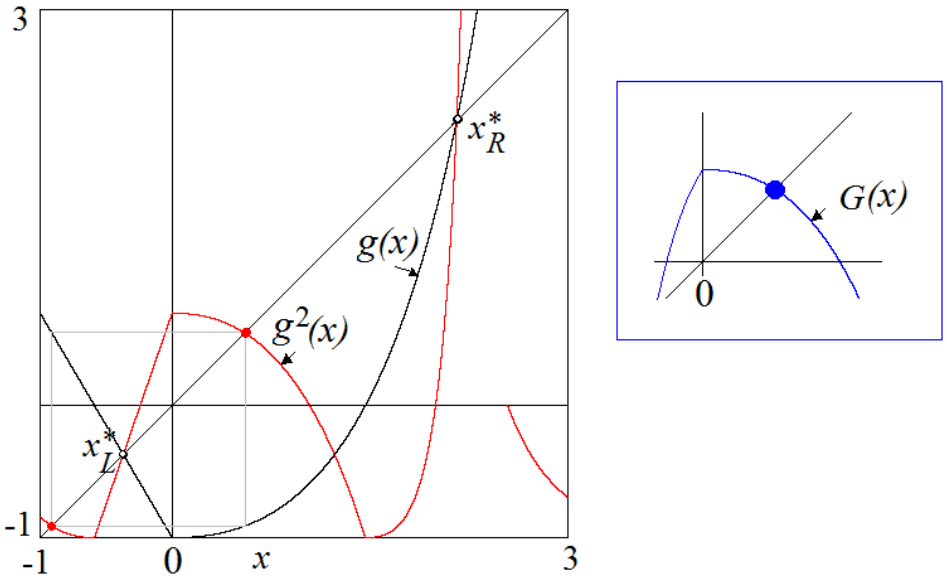

FIGURE 5. Maps $g(x)$ and $g^2(x)$ at $a = -1.7$, $b = 10$ and $\gamma = 1.5$. In the right panel the generic case starting a period doubling sequence is schematically shown.

having the positive derivative close to 0 at the periodic point on the right side of $x = 0$, thus leading to an attracting 2-cycle LM. Fig.5 shows an enlargement of Fig.3b, where besides map g also map g^2 is presented (for which the 2-cycle LM corresponds to two attracting fixed points).

Thus, as long as this unique 2-cycle of map $g(x)$ is attracting, it attracts all the points in J except for the fixed point x_L^*. This corresponds to the 3-cycle LR^2 of

map f, which attracts all the points, except for x_L^* and x_R^* and their preimages. The 3-cycle of f is not related to a fold bifurcation, and thus it does not exist a companion repelling cycle, because for map g the 2-cycle LM is born (decreasing a through -1) at the DFB of x_L^* at $a=-1$.

Decreasing the parameter a, the ranges $a_R^h < a < -1$, $a_{LR^3} < a < a_R^h$ and $a < a_{LR^3}$, are related to different dynamic properties. In the following subsections we describe the dynamics occurring in the first range, for $a \in (a_R^h, -1)$, where the use of map g is very convenient. In particular, we can explain how the first cascade of flip bifurcations in map g leads to attracting cycles of map f of periods 3, 6, 11, 22, 43, 86, ... (see Fig.4).

As stated in Property 2, for any fixed value $b>0$ in the range $a \in (a_R^h, -1)$ (where a_R^h and b satisfy the equation of the homoclinic bifurcation b_R^h given in (25)), the asymptotic dynamics of map g involve only the symbols L and M since it holds that $f_L(-1) < x_R^*$, and dynamics are confined in the invariant absorbing interval $J=[-1,-1-a] \subset [-1, x_R^*]$, inside which map g is continuous and unimodal.

Even if g is not smooth, the bifurcations occurring in the considered parameter range can be completely described. In fact, when the parameter a is decreased, the attracting cycles of map g appear in the order described by the well known U-sequence for a unimodal map (see e.g. [20]). In particular, at $a=a_R^h$ all the cycles from the U-sequence exist and are repelling.

We know that in smooth maps the U-sequence is characterized by fold bifurcations (which open periodic windows) and cascades of period doubling bifurcations. In map g the critical point $x=0$ is a kink point, and, thus, the fold bifurcation in J may be either standard S-fold bifurcations or fold-BCBs, leading to a pair of cycles, one of which is necessarily repelling. We shall prove that for the considered parameter range the second cycle is necessarily attracting. Similarly, in the cascade of period-doubling bifurcations, it is possible to observe both standard S-flip bifurcations and flip-BCBs. First we discuss a cascade originating by a 2-cycle born via the DFB at $a=-1$ (see Sec. 3.1.1). Then we generalize the result proving (in Sec.3.1.2) the following

Proposition 6. *Let $b>0$ and $\gamma>1$ be fixed, and $a \in (a_R^h, -1)$, where $a=a_R^h$ satisfies the condition $b=b_R^h$ given in (25) of the first homoclinic bifurcation of x_R^*, then*

- *any fold bifurcation (either fold-BCB or S-fold) of map g given in (21) is associated with the appearance of a pair of cycles of map f, one attracting and one repelling, whose periods differ by 1 (say n and $n-1$).*
- *Let $x=x^*>0$ be a periodic point, closest to $x=0$, of an attracting n-cycle of f with a negative eigenvalue, which attracts all the points of the interval $(0,x^*)$, and let $R^2\widetilde{\rho}_0$ be the symbolic sequence of this cycle (here $\widetilde{\rho}_0$ stands for the remaining symbolic sequence, necessarily starting with L). Then, decreasing a it is observed a cascade of alternating S-flip bifurcations and border collisions (BCs) leading to attracting cycles whose symbolic sequences can be written as $R^2\widetilde{\rho}_k$, where $\widetilde{\rho}_k = \widetilde{\rho}_{k-1} T \widetilde{\rho}_{k-1}$, $k=1,2,...$, with the alternating symbols $T=R^2$ and $T=L$. The symbol $T=R^2$ corresponds to an S-flip bifurcation, so that an attracting m-cycle in this cascade is followed by an attracting $2m$-cycle, while the symbol $T=L$ is associated with a BC and the m-cycle is followed by an attracting $(2m-1)$-cycle.*

For example, starting from an attracting n-cycle with symbolic sequence $R^2\widetilde{\rho}_0$ undergoing an S-flip bifurcation, one can observe the following cascade:

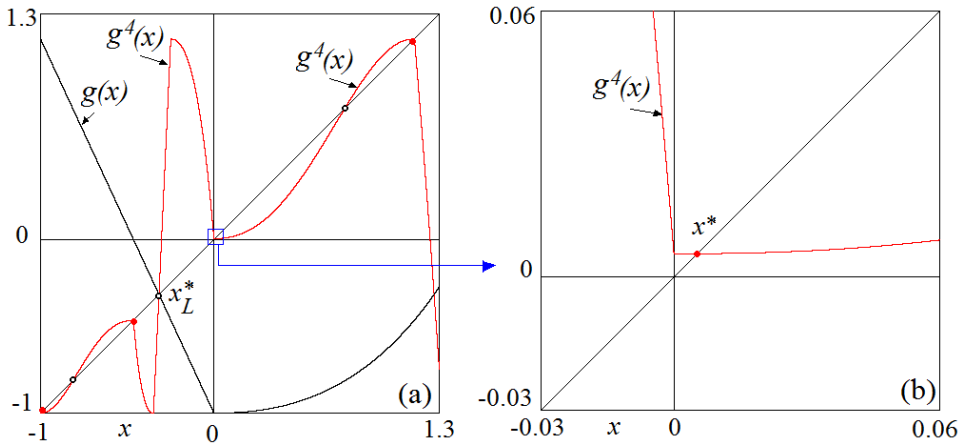

FIGURE 6. Attracting 4-cycle $(ML)^2$ of map $g(x)$ corresponding to the 6-cycle R^2LR^2L of map $f(x)$. The cycle is close to its border collision. In (b) the enlargement of the small rectangle indicated in (a). Here $a = -2.155$, $b = 10$, $\gamma = 1.5$.

$$R^2\widetilde{\rho}_0 \overset{S-flip}{\Rightarrow} R^2\underbrace{\widetilde{\rho}_0 R^2\widetilde{\rho}_0}_{\widetilde{\rho}_1} \overset{BC}{\Rightarrow} R^2\underbrace{\widetilde{\rho}_1 L\widetilde{\rho}_1}_{\widetilde{\rho}_2} \overset{S-flip}{\Rightarrow} R^2\underbrace{\widetilde{\rho}_2 R^2\widetilde{\rho}_2}_{\widetilde{\rho}_3} \overset{BC}{\Rightarrow} R^2\underbrace{\widetilde{\rho}_3 L\widetilde{\rho}_3}_{\widetilde{\rho}_4} \Rightarrow \ldots \quad (27)$$

and the period p_i of a cycle related to this cascade is defined as $p_i = 2p_{i-1}$ for i odd, and $p_i = 2p_{i-1} - 1$ for i even, where $p_0 = n$.

3.1.1. *Cascade of S-flip and flip-BCB of the 2-cycle.* We already know that for $b > 0$ and $\gamma > 1$, decreasing the parameter a from -1 an attracting 2-cycle ML of map g appears due to a DFB which is also a BCB for the outermost 2-cycle $\{-1, 0\}$ of g (or f_L) existing at $a = -1$ in the invariant interval $[-1, 0]$ filled with 2-periodic points. If we continue to decrease a the eigenvalue of the 2-cycle ML approaches -1. As map g^2 is smooth at the two corresponding fixed points, this first flip bifurcation is a standard one, S-flip. That is, decreasing the value of a the two fixed points of g^2 become repelling and an attracting 2-cycle appears in a neighborhood of each repelling fixed point, leading to an attracting 4-cycle $(ML)^2$ for map g. This bifurcation is also a pitchfork bifurcation for map g^4 leading to 4 attracting fixed points. Considering the fixed point of g^4 closest to the kink point on its right side, say $x^* > 0$, we have that decreasing a the local minimum decreases, this fixed point x^* approaches $x = 0$ and undergoes a BC at some value (which in smooth maps corresponds to the crossing of the critical point, associated with superstable cycles), at which x^* collides with $x = 0$.

As an example, for the parameter values related to Fig.5 we show the attracting 2-cycle ML of map g and the two attracting fixed points of g^2. One can see that the derivative at the periodic points is close to -1, i.e. the parameters are close to the flip bifurcation value of the 2-cycle. In Fig.6 we show the map g^4 before the BC, and the point $x^* > 0$ in the enlargement of Fig.6b.

The result of this BC can be predicted by using the skew tent map as a normal form (as described for example in [32]). In fact, evaluating left- and right side

derivatives of the function at the kink point $x = 0$ one obtains two values:

$$\alpha = \lim_{x\to 0_-} \frac{d}{dx} g^n(x), \quad \beta = \lim_{x\to 0_+} \frac{d}{dx} g^n(x) \tag{28}$$

where $n = 4$. Then the point (α, β) in the 2D bifurcation diagram of the skew tent map with minimum (slope $\alpha < 0$ on the left side and $\beta \geq 0$ on the right one), determines the result of the collision. Due to Property 1 we have that it always holds that $\beta = 0$. This simplifies the analysis, as there are only two possibilities: the border collision is either (i.1) *flip-BCB* or (i.2) *persistence-BC*, occurring as follows:

(i.1) If $\alpha \leq -1$ then the bifurcation is a *flip-BCB* (leading to a cycle of double period). That is, after the collision the fixed point x^* of g^4 belongs to the left side, i.e. $x^* < 0$, and becomes repelling, while an attracting 2-cycle of g^4 appears, with periodic points on the opposite sides of $x = 0$ (attracting fixed points of g^8 related to an attracting 8-cycle of g).

(i.2) If $-1 < \alpha < 0$ then a *persistence-BC* is observed. That is, after the collision the fixed point x^* of g^4 belongs to the left side, i.e. $x^* < 0$, and persists as attracting. The eigenvalue of the attracting 4-cycle of map g becomes negative, i.e. the slope of g^4 at $x^* < 0$ is negative. As a is decreased further an *S-flip bifurcation* must occur, leading to an attracting 2-cycle of g^4 (constituting an attracting 2^3-cycle of map g). Then the periodic point of the attracting cycle closest to the kink point on the left side collides with it, and another *persistence-BC* occurs (since the cycle is attracting one slope is larger than -1 and the other is 0), leading to an attracting 2^3-cycle of map g with different symbolic sequence.

Notice that independently on the occurrence of (i.1) or (i.2) the ultimate result of the bifurcation sequence described above is the same, as summarized in the following diagram for the symbolic sequences of the cycles of map g:

$$\begin{array}{lll}
ML \text{ attr.} \overset{S-flip}{\rightarrow} & & \\
\quad ML \textit{ rep.} & & \\
\quad MLML \text{ attr.} & \text{(i.1)} \overset{flip-BCB}{\rightarrow} & LLML \textit{ rep.} \\
 & & (MLML)LLML \textit{ attr.} \\
\quad ML \textit{ rep.} & & \\
\quad MLML \text{ attr.} & \text{(i.2)} \overset{BC}{\rightarrow} & \text{(persist.-BC) } LLML \text{ attr.} \\
 & & \text{(S-flip) } LLML \textit{ rep.} \text{ (and } (LLML)^2 \text{ attr.)} \\
 & & \text{(persist.-BC) } (MLML)LLML \textit{ attr.}
\end{array}$$

In the example considered above it holds $\alpha < -1$ and thus a flip-BCB occurs (case (i.1)), as shown in Fig.6, Fig.7 and the enlargements. The enlargement in Fig.7b also shows the local shape of the function g^8.

Considering the fixed point $\overline{x}^*$ of g^8 closest to $x = 0$ on the right side, one can see that the map has negative slope at this point. Decreasing the parameter a the bifurcation sequence is repeated: first an S-flip bifurcation of this point leads to a 2^4-cycle of map g, then a BC (either (i.1) or (i.2)) occurs.

In our example, the periodic point closest to $x = 0$ on its right side collides with $x = 0$, with derivatives $\beta = 0$ on the right side and $\alpha < -1$ on the left side, leading to a flip-BCB which gives an attracting 2^5-cycle of map g, and so on. The full cascade occurs, with alternating S-flip and flip-BCB, leading to attracting cycles of doubled periods for map g. Note that this cascade occurs in a very narrow interval of values of the parameter a.

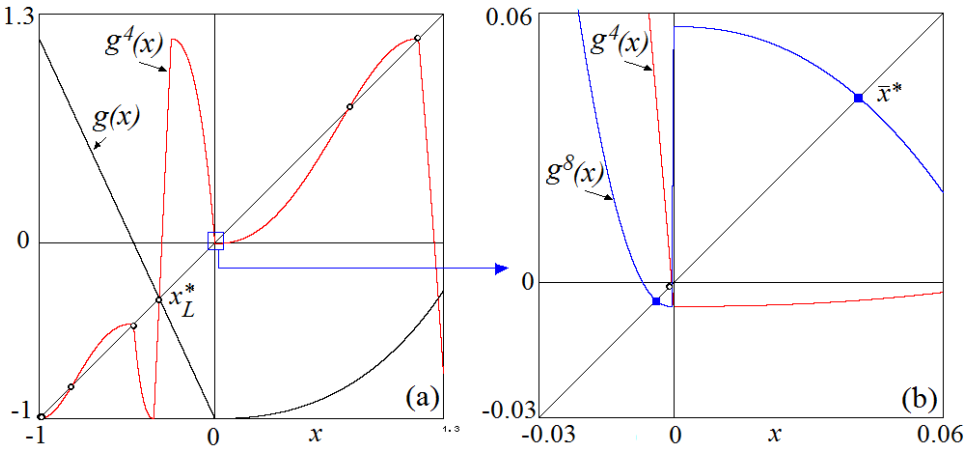

FIGURE 7. In (a), repelling 4-cycle ML^3 of map g corresponding to the repelling 5-cycle R^2L^3 of map f. In (b), the enlargement of the small rectangle marked in (a), which shows also the graph of $g^8(x)$ with an attracting 8-cycle $L^2(LM)^3$ of map g corresponding to the attracting 11-cycle $L^2(LR^2)^3$ of map f. Here $a = -2.16$, $b = 10$, $\gamma = 1.5$.

As we have already mentioned, this sequence of bifurcations for the original map f is very peculiar. In fact, the 2-cycle ML of map g corresponds to the 3-cycle R^2L of map f and its S-flip bifurcation leads to the attracting 6-cycle $(R^2L)R^2L$ of map f. But then, the attracting 6-cycle of f undergoes a BC from the right side (a periodic point collides with $x = 0$ from the right side, and thus its image collides with $+\infty$) after which, i.e. decreasing a, after the crossing of the kink point, it becomes a repelling 5-cycle R^2L^3 of map f, while the attracting 11-cycle $L^2(R^2L)^3$ of map f appears. The symbolic sequences of the cycles of map f are summarized in the following diagram:

$$R^2L \text{ attr.} \overset{S-flip}{\rightarrow} \begin{array}{l} R^2L \textit{ rep.} \\ R^2LR^2L \text{ attr.} \quad \text{(i)} \overset{BC}{\rightarrow} \begin{array}{l} LLR^2L \textit{ rep.} \\ (R^2LR^2L)LLR^2L \textit{ attr.} \end{array} \end{array}$$

This peculiar transition of the 6-cycle of f into a 5-cycle is due to the BC which involves infinity. In fact, the attracting 6-cycle $(R^2L)R^2L$ has periodic points which at the BC tend to the values $\{0, +\infty, -1, R, R, L\}$ that means for f the 5-cycle $\{0, -1, R, R, L\}$, and after the BC the periodic point in 0 moves to the left side, so that the repelling cycle which is left after the collision has symbolic sequence $\{L, L, R, R, L\}$. It follows that for map f the bifurcation sequence leads (alternatingly) to cycles with double period, say, $2m$, when it is an S-flip and to cycles of period $2m - 1$ when it is a BC.

This explains the sequence of periods of the attracting cycles, which is observed in Fig.4a starting from the attracting 3-cycle of map f, namely, the periods 3, 6, 11, 22, 43, ... We can also notice that the cascade which starts from the attracting 5-cycle of map f consists of the attracting cycles with periods 5, 10, 19, 38, 76, ... and so on. In fact, the mechanism described above can be generalized.

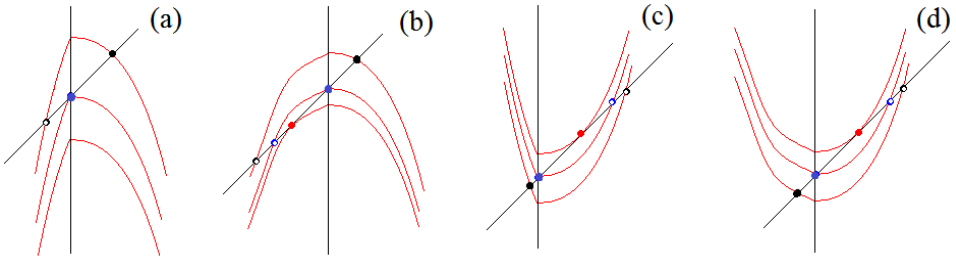

FIGURE 8. Qualitative representation of the S-fold and BCBs of map g^n in a neighborhood of $x = 0$, in all the possible cases, showing the shape of g^n at the bifurcation and after: In (a) a fold-BCB; in (b) an S-fold, related to a local maximum of g^n in $x = 0$; in (c) a fold-BCB; in (d) an S-fold, related to a local minimum of g^n in $x = 0$.

3.1.2. *Proof of Proposition 6 ($a \in (a_R^h, -1)$, $b > 0$, $\gamma > 1$).* Let us first consider the fold bifurcations (either S-fold or fold-BCB) initiating each new set of adjacent periodicity regions or, in other words, leading to the different "boxes" of the PWS map g. It is known that in unimodal PWS maps a fold-BCB may lead not only to one attracting and one repelling cycle, but also to two repelling cycles (as it may occur for example in the skew tent map). However, such a case can not occur in map g as can be shown making use of the skew tent map as a normal form.

Consider a fold bifurcation of a pair of n-cycles of map g. We can restrict our analysis to the n-th iterate of g, i.e., g^n, in a neighborhood of the kink point $x = 0$. A fold may be associated with a local maximum or a local minimum of g^n at $x = 0$, as qualitatively shown in Fig.8. We describe these cases separately.

Fold-BCB and S-fold related to a local maximum.

Let $x = 0$ be a local maximum of g^n, approaching the diagonal from below. It occurs, for example, at all the fold bifurcations leading to basic cycles MRM^k, for any $k \geq 1$. What matters are the slopes α and β on the right and left side of $x = 0$, respectively (see (28)). From Property 1 we know that g^n is locally flat on its right side, thus $\beta = 0$, while $g^n(x)$ must be monotone increasing on the left side of $x = 0$ so that $\alpha > 0$. Two cases, either $\alpha \geq 1$ or $0 < \alpha < 1$, are possible. By using the skew tent map as a normal form, we have that:

(j.1) if $\alpha \geq 1$ then a *fold-BCB* occurs (as shown as in Fig.8a);

(j.2) if $0 < \alpha < 1$ then an *S-fold* bifurcation occurs first (as shown as in Fig.8b), followed by a *persistence-BC*.

If $\alpha \geq 1$ then a contact with the diagonal must necessarily occur exactly in the kink point $x = 0$ (i.e. it cannot occur before), and thus it is a fold-BCB, leading to two fixed points of g^n on opposite sides of $x = 0$. For map g the symbolic sequences of the related n-cycles differ only in the first symbol, which are L and M, say with symbolic sequence $M\rho$ which is attracting and $L\rho$ which is repelling, where ρ represents a suitable sequence of symbols L and M, starting with the symbol L.

If $\alpha < 1$ then the contact with the diagonal must occur in smooth way, in a point on the left side of $x = 0$. That is, an S-fold bifurcation occurs, leading to two cycles having the same symbolic sequence, $L\rho$, where the fixed point on the left side of the tangency point is repelling and the other one, on the right, is attracting, so that

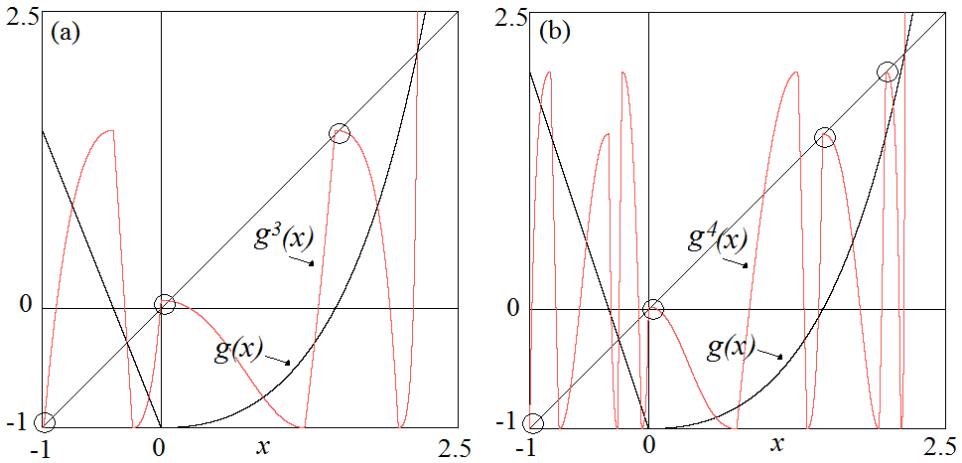

FIGURE 9. In (a): fold-BCB leading to a pair of 3-cycles of map g; In (b): fold-BCB leading to a pair of 4-cycles of map g. Here $a = -2.5$, $b = 10$, $\gamma = 1.5$.

the attracting cycle is the one closest to the origin. Thus, when the local maximum is increased, the attracting cycle undergoes a BC, and since it holds that $0 < \alpha < 1$ and $\beta = 0$, the collision leads to persistence of the attracting cycle, which however changes its symbolic sequence to $M\rho$.

In both cases, ultimately we have a pair of n-cycles of map g, one with symbolic sequence $L\rho$ which is repelling and $M\rho$ which is attracting. Map g has negative slope at the periodic point of the attracting cycle $M\rho$ on the right side of $x = 0$, as qualitatively shown in the rectangle in Fig.5, approaching an S-flip bifurcation. For the map $G(x) = g^n(x)$ a sequence of attracting cycles of doubled period is initiated, as the parameter a decreases, via alternating S-flip and BC, as explained below.

It is worth to note that these fold bifurcations are particular when referred to map f. In fact, ultimately in both cases the bifurcation leads to a pair of cycles whose periods differ by 1, an attracting cycle with symbolic sequence $R^2\widetilde{\rho}$ (where $\widetilde{\rho}$ is obtained from ρ substituting M by R^2), and a repelling one with symbolic sequence $L\widetilde{\rho}$. This is due to the BC with singularity which involves infinity, as in the cases commented above.

Two examples of fold bifurcations of the basic cycles MRM^k for $k = 1$ and $k = 2$, which both are fold-BCB as in the case (j.1) described above, are shown in Fig.9. In Fig.9a we show map g and its third iterate g^3 at the parameter values soon after the fold-BCB leading to an attracting cycle MLM and a repelling one LLM. For map f this leads to the attracting 5-cycle R^4L (whose periodicity region is clearly visible in Fig.4a) and a repelling 4-cycle L^2R^2. In Fig.9b we show map g and its fourth iterate g^4 at the parameter values soon after the fold-BCB leading to an attracting cycle MLM^2 and a repelling one LLM^2. For map f this leads to the attracting 7-cycle R^6L (see the related periodicity region in Fig.4a), and a repelling 6-cycle L^2R^4.

BC and S-fold related to a local minimum.

If we consider a local minimum of g^n at $x = 0$, approaching the diagonal from above (see Fig.8.c,d), the fold bifurcation is necessarily smooth as g^n is locally flat

on its right side, thus an *S-fold* leads to a pair of cycles both with symbolic sequence $M\rho$ (where ρ represents a suitable sequence of symbols L and M, starting with L). The attracting cycle is the one closest to the origin, and the other one is repelling. Thus, as the minimum decreases the attracting cycle undergoes a *BC*, merging with $x = 0$ from the right side. For the slope α on the left side of $x = 0$ it holds that $\alpha < 0$, and the slope on the right side is $\beta = 0$. We have two cases: either $\alpha \le -1$ or $-1 < \alpha < 0$. By using the skew tent map as a normal form, it is easy to show that

(jj.1) if $\alpha < -1$ then a *flip-BCB* occurs, leading to a repelling cycle with symbolic sequence $L\rho$ and an attracting cycle of double period, with symbolic sequence $M\rho L\rho$;

(jj.2) if $-1 < \alpha < 0$ then a *persistence-BC* occurs first, leading to an attracting cycle $L\rho$, and as the minimum decreases the attracting cycle undergoes an *S-flip*, it becomes repelling leading to an attracting cycle of double period, with symbolic sequence $L\rho L\rho$. Then the periodic point closest to $x = 0$ from the left side undergoes a *persistence-BC*, leading to an attracting cycle with symbolic sequence $M\rho L\rho$.

In both cases, ultimately we have a repelling cycle $M\rho$, a repelling cycle $L\rho$ and an attracting cycle $M\rho L\rho$ of double period. In particular, considering the map g^{2n}, it has a local maximum at $x = 0$, and its slope is negative at the periodic point of the attracting cycle $M\rho L\rho$ on the right side of $x = 0$ (as qualitatively shown in the rectangle indicated in Fig.5) approaching an S-flip bifurcation. For the map $G(x) = g^{2n}(x)$ a sequence of attracting cycles of doubled periods is initiated, as the parameter a decreases, via alternating S-flip and BC, as explained below.

As in the previous case, it is worth to emphasize the peculiarity of the sequence of bifurcations in map f. The S-fold leads to a pair of cycles, one is attracting and one repelling, with symbolic sequence $R^2\widetilde{\rho}$, where $\widetilde{\rho}$ is obtained from ρ substituting M by R^2. The attracting cycle undergoes a BC and then ultimately, in both cases (jj.1) and (jj.2), the bifurcation leads to a pair of repelling cycles whose periods differ by 1, with symbolic sequence $R^2\widetilde{\rho}$ and $L\widetilde{\rho}$, plus an attracting cycle with symbolic sequence $R^2\widetilde{\rho}L\widetilde{\rho}$. Note that for map f, independently on the symbols in $\widetilde{\rho}$, the period of this attracting cycle is necessarily *odd*, and the periodic point closest to $x = 0$ on the right side, say x^*, attracts all the points of the interval $(0, x^*)$, and thus a flip bifurcation can occur as a decreases.

The difference in the periods of the two repelling cycles is due to the BC with singularity which involves infinity: when a k-cycle of map f with a periodic point in the R side close to 0, and thus with symbolic sequence $R^2L...$, undergoes a BC, its periodic points tend to $\{0, +\infty, -1, ...\}$, that also means for f the cycle $\{0, -1, ...\}$, whose period is decreased by 1, that is, $k - 1$.

Cascade of S-flip and BC for a generic cycle

Consider now a generic attracting m-cycle of map g with negative eigenvalue, and let $x^* > 0$ be the fixed point of g^m closest to $x = 0$, which attracts all the points of the interval $(0, x^*)$. For example, after a fold bifurcation related to local extremum in $x = 0$ as described above, we consider g^n at a local maximum and g^{2n} at a local minimum. Let us denote by $M\rho_k$ symbolic sequence of the m-cycle, where ρ_k starts with L. Locally the graph of g^m is as in the rectangle shown in Fig.5, and we can reason as it is done for the 2-cycle of g (corresponding to the simplest case $\rho_k = L$, although the appearance of the 2-cycle is not related to a fold bifurcation). As the parameter a decreases, the sequence starts with an S-flip, leading to repelling cycle $M\rho_k$ and an attracting cycle $M\rho_k M\rho_k$ of double period. Then the periodic point

closest to $x = 0$ on its right side undergoes a BC, and what matters are the slopes α and β on the right and left side, respectively, of the function g^{2m} at the critical point $x = 0$, at the collision (the slopes are given in (28) with $n = 2m$). We have two cases:

(ii.1) If $\alpha \leq -1$ then the a *flip-BCB* occurs. That is, after the collision the considered fixed point of g^{2m} crosses $x = 0$ and belongs to the left side becoming repelling with symbolic sequence $L\rho_k M\rho_k$, while an attracting 2-cycle of g^{2m} appears, with periodic points on the two sides of $x = 0$, which for map g is a cycle with symbolic sequence $(M\rho_k M\rho_k)L\rho_k M\rho_k$.

(ii.2) If $-1 < \alpha < 0$ then a *persistence-BC* occurs. That is, after the collision the fixed point of g^{2m} belongs to the left side (which is the $2m$-cycle $L\rho_k M\rho_k$ for g), and persists as attracting. Moreover, in this case the eigenvalue of the attracting $2m$-cycle of map g becomes negative, and as a is decreased further an *S-flip bifurcation* must occur, leading to an attracting $4m$-cycle of map g with symbolic sequence $(L\rho_k M\rho_k)L\rho_k M\rho_k$. After this bifurcation the periodic point closest to $x = 0$ on the left side (fixed point of g^{4m}) collides with $x = 0$ from the left side, leading necessarily to a *persistence-BC* (as the slopes on both sides are one 0 and the other smaller than 1 in modulus). Then this attracting fixed point of g^{4m} moves to the right side, leading to an attracting $4m$-cycle for map g with symbolic sequence $(M\rho_k M\rho_k)L\rho_k M\rho_k$.

Notice that independently on the occurrence of (ii.1) or (ii.2) the ultimate result of the existing attracting and repelling cycles is the same, as summarized in the following diagram for the symbolic sequences of the cycles of map g:

$$
\begin{array}{l}
M\rho_k \text{ attr. } \overset{S-flip}{\to} \\
\qquad \begin{array}{l}
M\rho_k \text{ rep.} \\
M\rho_k M\rho_k \text{ attr.} \quad \text{(ii.1)} \overset{flip-BCB}{\to} \quad \begin{array}{l} L\rho_k M\rho_k \text{ rep.} \\ (M\rho_k M\rho_k)L\rho_k M\rho_k \text{ attr.} \end{array} \\
\\
M\rho_k \textit{ rep.} \\
M\rho_k M\rho_k \text{ attr.} \quad \text{(ii.2)} \overset{BC}{\to} \quad \begin{array}{l} \text{(persist.-BC) } L\rho_k M\rho_k \text{ attr.} \\ \text{(S-flip) } L\rho_k M\rho_k \textit{ rep.}, (L\rho_k M\rho_k)^2 \text{ attr.} \\ \text{(persist.-BC) } (M\rho_k M\rho_k)L\rho_k M\rho_k \textit{ attr.} \end{array}
\end{array}
\end{array}
$$

We can summarize the cascade of period-doubling bifurcations of any m-cycle of map g by use of the following mechanism. Let $M\rho_0$ be the symbolic sequence of an attracting cycle (for example the one born due to a fold bifurcation), where ρ_0 stands for the remaining symbolic sequence starting with L (in the case of the 2-cycle occurring as a is decreasing from -1, it is $\rho_0 = L$), then for decreasing a we have alternating S-flip and BC leading to cycles whose symbolic sequences can be written as follows, starting from $k = 0$:

$$
\begin{array}{l}
M\rho_k \text{ attr. } \overset{S-flip}{\to} \\
\qquad \begin{array}{l}
M\rho_k \textit{ rep.} \\
M\rho_{k+1} \textit{ attr. } \rho_{k+1} = \rho_k M\rho_k \quad \text{(ii)} \overset{BC}{\to} \quad \begin{array}{l} L\rho_{k+1} \textit{ rep.} \\ M\rho_{k+2} \textit{ attr. } \rho_{k+2} = \rho_{k+1} L\rho_{k+1} \end{array}
\end{array}
\end{array}
$$

i.e. the attracting cycles of map g have symbolic sequence $M\rho_0$, $M\rho_1$, $M\rho_2$, $M\rho_3$, ... where the updating of the symbolic sequence of the cycles of doubled periods $\rho_{k+1} = \rho_k T\rho_k$ occurs with the symbol $T = M$ and $T = L$ alternatingly.

Similarly we can write the symbolic sequences for map f. Starting from $k = 0$, the attracting cycles of map f have the symbolic sequences $R^2\widetilde{\rho}_k$ where $\widetilde{\rho}_k$ (which starts with L) is obtained from ρ_k substituting M by R^2, and in the updating sequence $\widetilde{\rho}_{k+1} = \widetilde{\rho}_k T \widetilde{\rho}_k$ the symbol $T = R^2$ and $T = L$ alternate. Thus when $T = R^2$ (when the S-flip occurs) the period is doubled, say, $2m$, while when $T = L$ (i.e. the BC occurs) the period is $2m - 1$.

We have so proven Proposition 6.

3.1.3. *Unbounded chaotic intervals for $a \in (a_R^h, -1)$.* Let us discuss other properties of map f given in (2) making use of the continuous unimodal map g defined in the interval J (see (5)). In particular, it holds that all the cycles of map g, except for the fixed points, have even periods as long as the fixed point x_L^* is not homoclinic. The *first homoclinic bifurcation* of x_L^* occurs when $f_M \circ f_L(-1) = x_L^*$ leading to the following condition:

$$b_L^h: \quad \frac{b}{(b(-a-1)^{-\gamma}-1)^{\gamma}} = \frac{a}{a-1} \tag{29}$$

More relevant is the fact that for the considered parameter range, for any fixed $b > 0$ and a varying in the interval $(a_R^h, -1)$ there are open intervals dense in $[a_R^h, -1]$ related to attracting cycles. However, the set of values of a in the interval $(a_R^h, -1)$ at which map g has chaotic attractors (which are chaotic intervals with dense periodic points and aperiodic trajectories) is most likely a totally disconnected set of positive Lebesgue measure (and, thus, such attractors do not persist under parameter perturbations), as it occurs in smooth maps with negative Schwarzian derivative (see e.g. [12], or [35] for a survey). This is because the values at which the fold and flip bifurcations occur are only slightly modified, but all these bifurcations take place (even if border collisions are involved) and thus also the values of a at which all the homoclinic bifurcations of the repelling cycles occur, exist also here, as it happens in smooth maps.

As mentioned above, attracting chaotic intervals of map g (and, thus, of map f) are structurally unstable. Moreover, it is worth to note that for map f such attractors are unbounded. In fact, for map g, which is continuous in J, the images of the kink point give the boundaries of the chaotic interval(s). If it is a unique interval then it necessarily coincides with the interval $J = [-1, -a-1]$, while if it consists of k-cyclic chaotic intervals then $c_i = g^i(0)$ for $i = 1, ..., 2k$ are the boundary points of the intervals, and $x = 0$ necessarily belongs to one of them, say to interval B_0. For map f this means that the discontinuity point always belongs to the chaotic intervals, and thus also $f(B_0 \cap I_R)$ belongs to the chaotic attractor. Given that $f_R(B_0 \cap I_R) = [x^+, +\infty)$ with $x^+ > x_R^*$, we have that for f the chaotic intervals are necessarily *acyclic and unbounded* (see e.g. [2]).

Clearly, a unique chaotic interval $J = [-1, -a-1]$ for map g exists at $a = a_L^h$ when the homoclinic bifurcation of x_L^* occurs (i.e. the parameters b and a_L^h satisfy the equation of b_L^h given in (29)), and map f has two chaotic intervals: $[-1, -a-1] \cup [f_R(-a-1), +\infty)$. At $a = a_R^h$ related to the homoclinic bifurcation of x_R^* (i.e. the parameters belong to the curve b_R^h given in (25)), g is chaotic in $J = [-1, -a-1] = [-1, x_R^*]$ and f is chaotic in the interval $[-1, +\infty) = [-1, -a-1] \cup [f_R(-a-1), +\infty)$. Thus, we can state the following

Property 3. *Let $b > 0$ and $\gamma > 1$. At any value $a \in [a_R^h, -1)$ at which g has attracting chaotic intervals, map f has attracting unbounded acyclic chaotic intervals.*

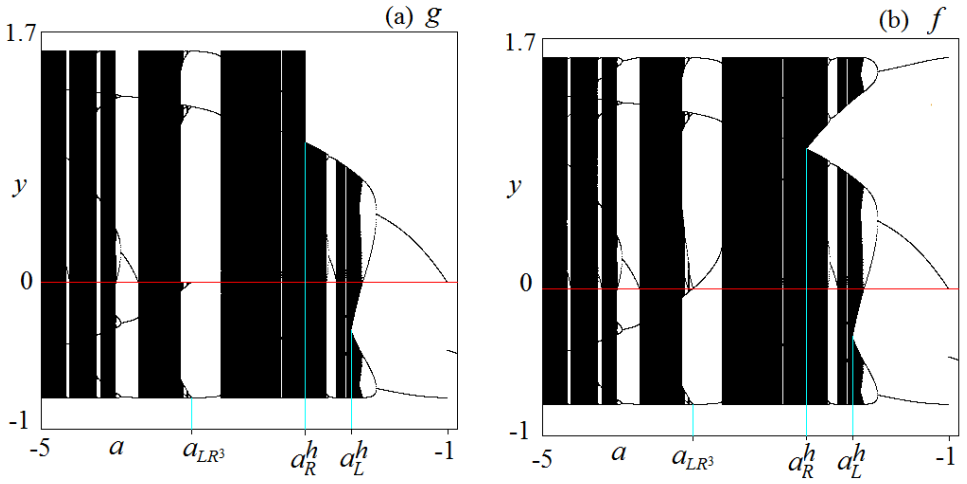

FIGURE 10. 1D bifurcation diagram as a function of a at $b = 4$, $\gamma = 1.5$ for map g in (a), and for map f in (b). The values of x are scaled as $y = \arctan(x)$ in order to show the values tending to $+\infty$.

Examples of 1D bifurcation diagrams for map g and map f are presented in Fig.10.

So, the dynamics related to the considered parameter range is well explained, however, this is not the case for $a < a_R^h$, as discussed in the next subsection.

3.1.4. *Other S-fold bifurcations for $a \le a_R^h$.* After the homoclinic bifurcation of the fixed point x_R^* map g is no longer unimodal in an invariant absorbing interval. Thus, map g or map f has to be considered in its complete range, which is $[-1, +\infty)$. Both maps, f and g, are discontinuous in the absorbing interval $[-1, +\infty)$ (with discontinuity points $x = 0$ and $x = O_R^{-1} = b^{\frac{1}{\gamma}}$, respectively), and fold bifurcations may occur in which f^n becomes tangent to the diagonal also at points larger than x_R^*. The occurrence of fold bifurcations is confirmed by Fig.4, where several periodicity regions of attracting cycles are evidenced, especially at large values of γ.

The bifurcation structure formed by the periodicity regions of attracting cycles existing for $a < a_R^h$ is still not well described. Below we give only some simple remarks leaving the detailed analysis of this structure for future study.

For any fixed value $b > 0$, in the range $a \in (a_{LR^3}, a_R^h)$ (where a_{LR^3} and b satisfy the equation of b_{LR^3} given in (26)), from the asymptotic dynamics of map g it follows that in the symbolic sequence of a trajectory of map f the symbol L is necessarily followed by at least three symbols R, that is, it includes LR^3. This is the reason why among the several periodicity regions existing in the considered parameter range, the last one (for decreasing a) is related to a 4-cycle LR^3, which appears by S-fold bifurcation involving two cycles with the same symbolic sequence, one attracting and one repelling.

The considered parameter range is confined by the values related to the BC of the attracting 4-cycle LR^3, detected at the beginning of Sec.3 (see (26)). At the bifurcation value ($a = a_{LR^3}$) there exists the attracting 4-cycle of f with periodic points $\{0, +\infty, -1, O_R^{-1}\}$ (applying f_R to $x = 0$) or also $\{0, -1, O_R^{-1}\}$ (applying f_L

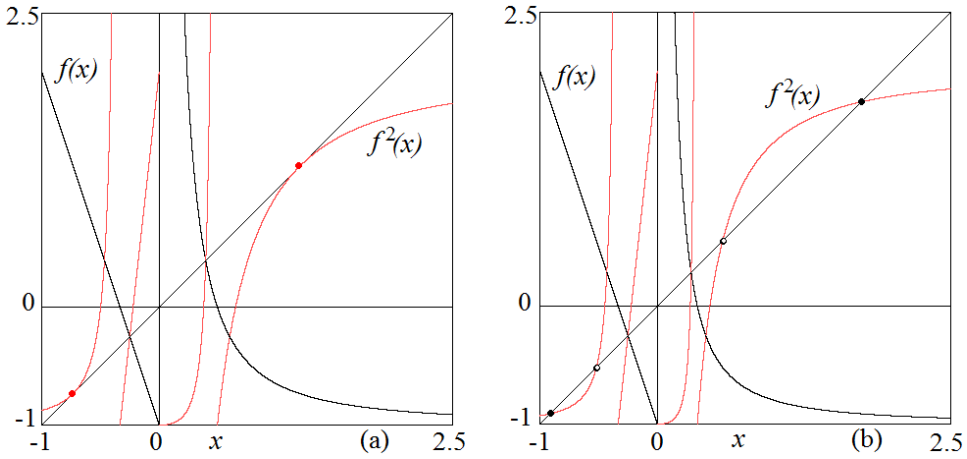

FIGURE 11. Fold bifurcation of the pair of 2-cycles LR at $a = -3$, $\gamma = 1.5$ and $b = 0.35$ in (a), $b = 0.2$ in (b).

to $x = 0$), and for $a < a_{LR^3}$ the BC of this attracting 4-cycle leads to a repelling 3-cycle with symbolic sequence L^2R.

For $a < a_{LR^3}$ the sequence of symbols LRL is also allowed, both for map g and map f. Thus, periodicity regions of different attracting cycles may exist where the last one (for decreasing a) is related to a pair of 2-cycles LR with points one smaller than x_L^* and the other larger than x_R^*. To detect this S-fold let $\{x_{0,2}, x_{1,2}\}$ be the periodic points of a 2-cycle of map f with $x_{0,2} \in I_L$ and $x_{1,2} = f_L(x_{0,2}) \in I_R$. Consider the composite function

$$F_{LR}(x) := f_R \circ f_L(x) = \frac{b}{(ax-1)^\gamma} - 1 \tag{30}$$

whose derivative is $F'_{LR}(x) = -ab\gamma(ax-1)^{-\gamma-1}$. The S-fold bifurcation is obtained solving both $F_{LR}(x) = x$ and $F'_{LR}(x) = 1$, leading to $x_{0,2} = \frac{1-a\gamma}{a(1+\gamma)}$ and the fold bifurcation curve

$$\varphi_{LR}: \quad b = -\frac{1}{a\gamma}\left(-\gamma\frac{a+1}{\gamma+1}\right)^{\gamma+1} =: b_{LR} \tag{31}$$

This curve is marked in Fig.1 and Fig.4, bounding the periodicity region of the 2-cycle LR. Clearly, also a repelling 2-cycle with the same symbolic sequence exists. An example of the occurring fold bifurcation is shown in Fig.11. The pair of 2-cycles exists for any parameter values (a, b) belonging to the region between the curve φ_{LR} and the axis $b = 0$.

Notice that the results obtained above for the fold bifurcation of a 2-cycle LR hold for any $\gamma > 0$ and thus the S-fold bifurcation curve given in (31) is related to a pair of cycles both for $\gamma > 1$ and $0 < \gamma \leq 1$. Thus, we can state the following

Proposition 7 (S-fold bifurcation of 2-cycle LR for $b > 0$)**.** *Let $a < -1$ and $\gamma > 0$, then at $b = b_{LR}$ where b_{LR} is given in (31), an S-fold bifurcation occurs. For $0 < b < b_{LR}$ a pair of 2-cycles of map f with symbolic sequence LR exist, one attracting and one repelling.*

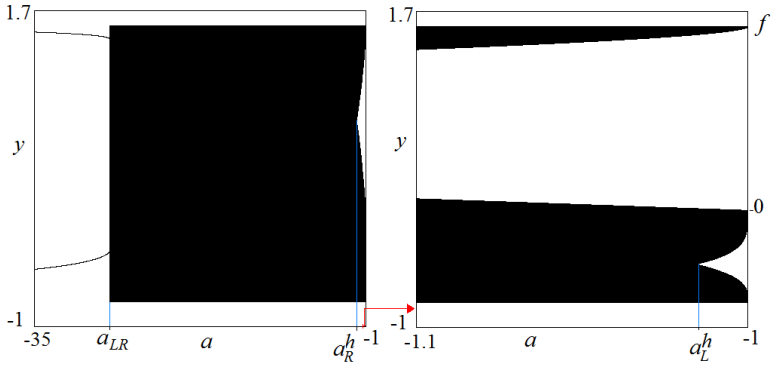

FIGURE 12. 1D bifurcation diagram of map f as a function of a at fixed $b = 1.9$ and $\gamma = 0.5$. The variable x is scaled by $y = \arctan(x)$. In (b) an enlargement of (a) is shown for $-1.1 < a < -1$.

The boundaries φ_{LR} marked in Fig.1 and Fig.4 are plotted using the equation given in (31). In particular, the curve φ_{LR} intersects the straight line $b = b_{LR}^f$ (in the figures mentioned above the intersection point is out of the window), thus there is a bistability region related to the attracting fixed point x_R^* and the attracting 2-cycle LR .

3.2. **Dominant chaos for $a < -1$, $b > 0$, $0 < \gamma < 1$.** For $-1 < a < 0$ the dynamics of f are characterized by convergence to fixed points, while for $a < -1$ the dynamics abruptly become chaotic, as can be seen in Fig.4a where the white region is related mainly to chaos. In fact, at $a = -1$ the DFB of x_L^* occurs, and for $a < -1$ an invariant chaotic set necessarily exists, attracting or repelling. We have different dynamic behaviors depending on the value of b, that is, depending on the existence of a repelling ($0 < b \le b_R^f$) or attracting ($b > b_R^f$) fixed point x_R^*, as described below.

3.2.1. *Chaos and a repelling fixed point x_R^*.* For any fixed value $b \in (0, b_R^f]$ (so that x_R^* is repelling) and $a_R^h < a < -1$, we can restrict the asymptotic dynamics to the interval J which is invariant for map g. Decreasing the value of a from -1, as long as the fixed point x_L^* is not homoclinic the invariant intervals of g are given by $[g(0), g^3(0)] \cup [g^4(0), g^2(0)] = [-1, f_R^2(-a-1)] \cup [f_L \circ f_R^2(-a-1), -a-1]$. Then at the parameter value related to the homoclinic bifurcation of x_L^* the invariant interval of g becomes $[g(0), g^2(0)] = [-1, -a-1]$, which persists up to the homoclinic bifurcation of x_R^*. Since it holds that $|g'(x)| > 1$ for any $x \in J$, an attracting cycle cannot exist, and due to the large slope of the function at the right side of the kink point (see Property 1), we can expect that map g really is chaotic in these invariant intervals.

For $a < a_R^h$ we have to consider map f in the interval $[-1, +\infty)$, and even if it holds that $|g'(x)| > 1$ for any $x \in [-1, O_R^{-1}]$, there are points with slope smaller than 1 in modulus for $x > O_R^{-1}$, thus attracting cycles may exist. This depends on the value of b. An example of the 1D bifurcation diagram is presented in Fig.12 for $\gamma = 0.5$ and $b = 1.9 < b_R^f = 2$ showing that the interval $[-1, +\infty)$ looks like an unbounded chaotic attractor for any $a \in (a_{LR}, a_R^h]$ (here a_{LR} is the value of a correspondinng b_{LR}). However, for example, at $\gamma = 0.5$ and $b = 0.1$, for

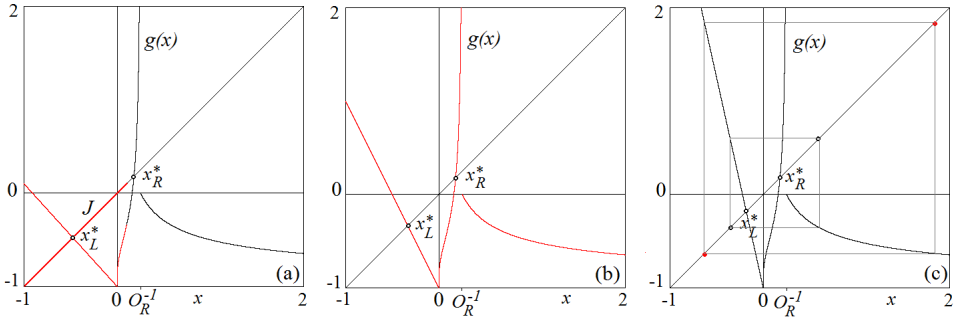

FIGURE 13. Graphs of map $g(x)$ at $\gamma = 0.5$ and $b = 0.5 < b_R^f$. In (a) $a = -1.1$; in (b) $a = -2$; in (c) $a = -4.5$.

$a \in (-1.25, -1.248)$ an attracting 4-cycle of map f exists, with symbolic sequence RL^3. Thus, attracting cycles of f may appear also for $a > a_{LR}$, before the crossing of the S-fold bifurcation curve φ_{LR}. So, as long as $a > a_{LR}$ the unbounded interval $U = [-1, +\infty)$ may be a chaotic attractor of map f, or it may include a chaotic repeller. Thus, we can state the following

Property 4 (robust unbounded chaos)**.** *Let $0 < \gamma < 1$ and $0 < b \le b_R^f$ then*

(1) for $a_L^h < a < -1$ map f has an unbounded chaotic attractor consisting of three intervals: $[-1, f_R^2(-a-1)] \cup [f_L \circ f_R^2(-a-1), -a-1] \cup [f_R(-a-1), +\infty)$;

(2) for $a_R^h < a \le a_L^h$ map f has an unbounded chaotic attractor consisting of two intervals: $[-1, -a-1] \cup [f_R(-a-1), +\infty)$;

(3) for $a_{LR} < a \le a_R^h$, depending on the value of b, map f has either an unbounded chaotic attractor $[-1, +\infty)$ *or an unbounded chaotic repellor;*

(4) for $a < a_{LR}$ almost all trajectories converge to the attracting 2-cycle born crossing the curve φ_{LR}, and a chaotic repeller exists.

Examples of map g in the cases 2, 3 and 4 listed in Property 4 are shown in Fig.13.

3.2.2. *Chaos and an attracting fixed point x_R^*.* Differently from the previous case, for any fixed value $b > b_R^f$, decreasing the parameter a from -1, x_R^* is an attracting fixed point of map g (and thus of map f) and two repelling fixed points of map g exist, x_{RR}^1 and x_{RR}^2, which are periodic points of a repelling 2-cycle of map f, bounding the immediate basin of x_R^*. However, as long as $f_L(-1) < x_{RR}^1$ (one can consider the related interval of values of a), there is coexistence of an invariant chaotic interval and the attracting fixed point. In fact, as long as the fixed point x_L^* is not homoclinic, the invariant intervals of g are given by $[g(0), g^3(0)] \cup [g^4(0), g^2(0)] = [-1, f_R^2(-a-1)] \cup [f_L \circ f_R^2(-a-1), -a-1]$. Then at the homoclinic bifurcation of x_L^* the invariant interval of g becomes $[g(0), g^2(0)] = [-1, -a-1]$, which persists up to the homoclinic bifurcation of x_{RR}^1. Let us denote a_{RR}^h the value of a at which this occurs. The invariant absorbing interval J includes a chaotic attractor of map g, as follows from the same arguments used above (since $|g'(x)| > 1$ for any $x \in J$, an attracting cycle cannot exist). The basin of attraction of the fixed point x_R^* is the union of the immediate basin (x_{RR}^1, x_{RR}^2) and its unique preimage $f_L^{-1}((x_{RR}^1, x_{RR}^2))$: $\mathcal{B}(x_R^*) = (x_{RR}^1, x_{RR}^2) \cup f_L^{-1}((x_{RR}^1, x_{RR}^2))$.

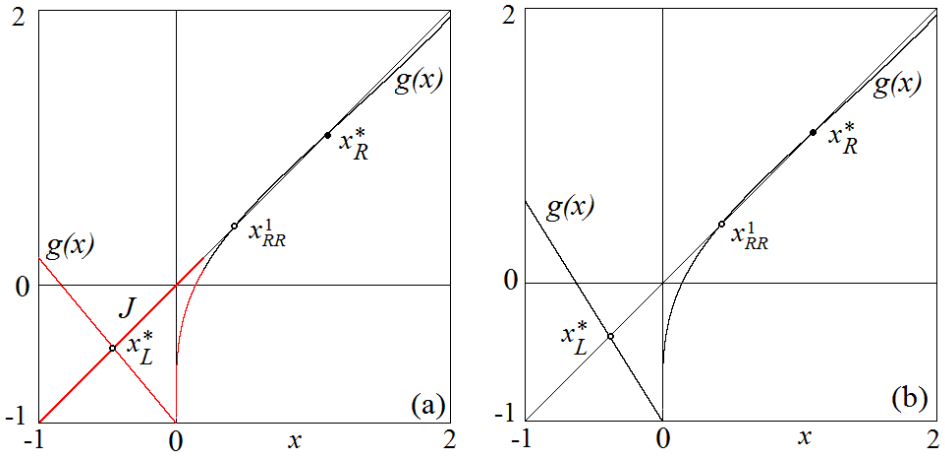

FIGURE 14. Graphs of map g at $\gamma = 0.5$ and $b = 2.2 > b_R^f$. In (a) $a = -1.2$; in (b) $a = -1.6$. The fixed point is the unique attractor.

For $a < a_{RR}^h$ a chaotic repeller exists in $[-1, +\infty)$. If x_R^* is the unique attractor, then it attracts almost all the points. However, a coexisting attracting cycle may appear (due to an S-fold bifurcation). For example this occurs for $a < a_{LR}$ when the attracting 2-cycle LR coexists with x_R^*. In such cases the chaotic repeller belongs to the boundary separating the two basins of attraction. We can so state the following

Property 5. *Let $0 < \gamma < 1$ and $b > b_R^f$ then*

(1) for $a_L^h < a < -1$ the attracting fixed point x_R^* of map f coexists with the unbounded chaotic attractor given by the intervals $[-1, f_R^2(-a-1)] \cup [f_L \circ f_R^2(-a-1), -a-1] \cup [f_R(-a-1), +\infty)$;

(2) for $a_{RR}^h < a \le a_L^h$ the attracting fixed point x_R^* of map f coexists with the unbounded chaotic attractor $[-1, -a-1] \cup [f_R(-a-1), +\infty)$;

(3) for $a_{LR} < a \le a_{RR}^h$ depending on the value of b, the fixed point x_R^* may be the unique attractor of map f, a chaotic repeller exists;

(4) for $a < a_{LR}$ the attracting fixed point x_R^* coexists with an attracting 2-cycle born due to an S-fold for parameter point crossing the curve φ_{LR}, and a chaotic repeller exists.

Examples of map g in the cases 2 and 3 of Property 5 are shown in Fig.14.

4. **Conclusions.** We have considered some bifurcations occurring in the 1D discontinuous linear-power map f defined in (1), where a, b, $\gamma > 0$ and $\mu < 0$ are real parameters. The bifurcations of the fixed points have been classified. As the dynamics are quite different depending on $b < 0$ and $b > 0$, we have considered these two different ranges separately. The case $a < 0$, $b < 0$ is related to an invertible map for which we have proved that particular sets of 2-cycles and 4-cycles are involved both in smooth and border collision bifurcations, leading to coexistence with an attracting fixed point. The case $a < 0$, $b > 0$ is associated with a noninvertible map, for which we have described quite a rich bifurcation structure of the parameter space emphasizing its dependence on γ. In particular, for $\gamma > 1$, when the repelling fixed point in the right partition is not homoclinic, we have shown

that fold bifurcations (either smooth fold or fold-BCB) ultimately lead to a pair of cycles of f, one attracting and one repelling, whose periods differ by 1. We have completely described, by using the skew tent map as a normal form, the peculiar sequences of alternating smooth flip bifurcations and border collision bifurcations starting from an attracting cycle of period n and followed by attracting cycles of periods $2n$, $(4n-1)$, $2(4n-1)$, $4(4n-1)-1$, ... The existence of unbounded chaotic attractors has been proved, which may be structurally unstable or robust. For $0<\gamma<1$, we have shown that as long as the fixed point in the right partition is repelling, map f has either an unbounded chaotic attractor, or an attracting cycle coexisting with a chaotic repeller on the boundary of its basin of attraction. Differently, when the fixed point in the right partition is attracting, it may coexist with an unbounded chaotic attractor or with some attracting cycle. Many problems related to the dynamics of the considered map are left open, which require further investigations.

Acknowledgments. The work of L. Gardini and I. Sushko has been performed under the auspices of the COST action IS1104 "The EU in the new economic complex geography: models, tools and policy evaluation", http://www.gecomplexity-cost.eu. L. Gardini acknowledge also the GNFM (National Group of Mathematical Physics, INDAM Italian Research Group). The second author would like to thank the assistance of Iran National Science Foundation (INSF) and Sharif University of Technology in supporting her postdoc program (Project Number: 95005034). I. Sushko thanks also University of Urbino for the hospitality during her stay there as a Visiting Professor.

REFERENCES

[1] F. Angulo and M. di Bernardo, Feedback control of limit cycles: A switching control strategy based on nonsmooth bifurcation theory, *IEEE Transactions on Circuits and Systems-I*, **52** (2005), 366–378.

[2] V. Avrutin, I. Sushko and L. Gardini, Cyclicity of chaotic attractors in one-dimensional discontinuous maps, *Mathematics and Computers in Simulation*, **95** (2014), 126–136.

[3] V. Avrutin, P. S. Dutta, M. Schanz and S. Banerjee, Influence of a square-root singularity on the behaviour of piecewise smooth maps, *Nonlinearity*, **23** (2010), 445–463.

[4] M. di Bernardo, C. J. Budd, A. R. Champneys and P. Kowalczyk, *Piecewise-smooth Dynamical Systems: Theory and Applications,* Applied Mathematical Sciences 163, Springer-Verlag, London, 2008.

[5] M. di Bernardo, C. Budd and A. Champneys, Grazing, skipping and sliding: Analysis of the non-smooth dynamics of the dc-dc buck converter, *Nonlinearity*, **11** (1998), 859–890.

[6] M. di Bernardo, C. J. Budd and A. R. Champneys, Corner collision implies border-collision bifurcation, *Physica D*, **154** (2001), 171–194.

[7] M. di Bernardo, P. Kowalczyk and A. B. Nordmark, Bifurcations of dynamical systems with sliding: Derivation of normal-form mappings, *Physica D*, **170** (2002), 175–205.

[8] G.I. Bischi, C. Mira and L. Gardini, Unbounded sets of attraction, *International Journal of Bifurcation and Chaos*, **10** (2000), 1437–1469.

[9] H. Dankowicz and A. B. Nordmark, On the origin and bifurcations of stick-slip oscillations, *Physica D*, **136** (2000), 280–302.

[10] L. Gardini, I. Sushko, V. Avrutin and M. Schanz, Critical homoclinic orbits lead to snap-back repellers, *Chaos Solitons & Fractals*, **44** (2011), 433–449.

[11] C. Halse, M. Homer and M. di Bernardo, C-bifurcations and period-adding in one-dimensional piecewise-smooth maps, *Chaos, Solitons & Fractals*, **18** (2003), 953–976.

[12] M. Jakobson, Absolutely continuous invariant measures for one-parameter families of one-dimensional maps, *Commun Math Phys*, **81** (1981), 39–88.

[13] A. Kumar, S. Banerjee and D. P. Lathrop, Dynamics of a piecewise smooth map with singularity, *Physics Letters A*, **337** (2005), 87–92.

[14] Y. L. Maistrenko, V. L. Maistrenko and L. O. Chua, Cycles of chaotic intervals in a time-delayed Chua's circuit, *Int. J. Bifurcat. Chaos*, **3** (1993), 1557–1572.
[15] R. Makrooni and L. Gardini, *Bifurcation Structures in a Family of One-Dimensional Linear-Power Discontinuous Maps*, Gecomplexity Discussion Paper N.7, 2015, ISSN: 2409–7497. http://econpapers.repec.org/paper/cstwpaper/
[16] R. Makrooni, N. Abbasi, M. Pourbarat and L. Gardini, Robust unbounded chaotic attractors in 1D discontinuous maps, *Chaos, Solitons & Fractals*, **77** (2015), 310–318.
[17] R. Makrooni, F. Khellat and L. Gardini, Border collision and fold bifurcations in a family of piecesiwe smooth maps. Part I: Unbounded chaotic sets, *J. Difference Equ. Appl.,* **21** (2015), 660–695.
[18] R. Makrooni, F. Khellat and L. Gardini, Border collision and fold bifurcations in a family of piecesiwe smooth maps: divergence and bounded dynamics, *J. Difference Equ. Appl.,* **21** (2015), 791–824.
[19] R. Makrooni, L. Gardini and I. Sushko, Bifurcation structures in a family of 1D discontinuos linear-hyperbolic invertible maps, *Int. J. Bifurcation and Chaos,* **25** (2015), 1530039 (21 pages).
[20] N. Metropolis, M. L. Stein and P. R. Stein, On finite limit sets for transformations on the unit interval, *J Comb Theory*, **15** (1973), 25–44.
[21] A. B. Nordmark, Non-periodic motion caused by grazing incidence in an impact oscillator, *Journal of Sound and Vibration*, **145** (1991), 279–297.
[22] A. B. Nordmark, Universal limit mapping in grazing bifurcations, *Physical Review E*, **55** (1997), 266–270.
[23] A. B. Nordmark, Existence of priodic orbits in grazing bifurcations of impacting mechanical oscillators, *Nonlinearity*, **14** (2001), 1517–1542.
[24] H. E. Nusse and J. A. Yorke, Border-collision bifurcations including period two to period three for piecewise smooth systems, *Physica D*, **57** (1992), 39–57.
[25] H. E. Nusse and J. A. Yorke, Border-collision bifurcation for piecewise smooth one-dimensional maps, *Int. J. Bifurcation Chaos*, **5** (1995), 189–207.
[26] H. Nusse, E. Ott and J. Yorke, Border collision bifurcations: An explanation for observed bifurcation phenomena, *Phys. Rev. E*, **49** (1994), 1073–1076.
[27] Z. Qin, J. Yang, S. Banerjee and G. Jiang, Border collision bifurcations in a generalized piecewise linear-power map, *Discrete and Continuous Dynamical System, Series B*, **16** (2011), 547–567.
[28] Z. Qin, Z. Yuejing, J. Yang and Y. Jichen, Nonsmooth and smooth bifurcations in a discontinuous piecewise map, *Int. J. Bifurcation and Chaos*, **22** (2012), 1250112 (7 pages).
[29] W. T. Shi, C. L. Gooderidge and D. P. Lathrop, Viscous effects in droplet-ejecting capillary waves, *Phys. Rev. E,* **56** (1997), 41–57.
[30] I. Sushko, A. Agliari and L. Gardini, Bistability and bifurcation curves for a unimodal piecewise smooth map, *Discrete and Continuous Dynamical Systems, Serie B*, **5** (2005), 881–897.
[31] I. Sushko, A. Agliari and L. Gardini, Bifurcation structure of parameter plane for a family of unimodal piecewise smooth maps: border-collision bifurcation curves, *Chaos Solitons & Fractals*, **29** (2006), 756–770.
[32] I. Sushko and L. Gardini, Degenerate bifurcations and border collisions in piecewise smooth 1D and 2D maps, *Int. J. Bif. and Chaos*, **20** (2010), 2045–2070.
[33] I. Sushko, L. Gardini and K. Matsuyama, Superstable credit cycles and U-sequence, *Chaos Solitons & Fractals*, **59** (2014), 13–27.
[34] I. Sushko, V. Avrutin and L. Gardini, Bifurcation structure in the skew tent map and its application as a border collision normal form, *Journal of Difference Equations and Applications,* **22** (2016), 582–629.
[35] H. Thunberg, Periodicity versus chaos in one-dimensional dynamics, *SIAM Rev*, **43** (2001), 3–30.
[36] S. Wiggins, *Introduction to Applied Nonlinear Dynamical Systems and Chaos*, Springer-Verlag, New York, 2003.

Received September 2016; revised March 2017.

E-mail address: laura.gardini@uniurb.it
E-mail address: royamakrooni@mehr.sharif.edu
E-mail address: sushko@imath.kiev.ua